Density Model for Bryde's Whale (*Balaenoptera edeni*) for the U.S. Gulf of Mexico: Supplementary Report

Duke University Marine Geospatial Ecology Lab*

Model Version 3.1 - 2015-11-06

Citation

When referencing our methodology or results generally, please cite our open-access article:

Roberts JJ, Best BD, Mannocci L, Fujioka E, Halpin PN, Palka DL, Garrison LP, Mullin KD, Cole TVN, Khan CB, McLellan WM, Pabst DA, Lockhart GG (2016) Habitat-based cetacean density models for the U.S. Atlantic and Gulf of Mexico. Scientific Reports 6: 22615. doi: 10.1038/srep22615

To reference this specific model or Supplementary Report, please cite:

Roberts JJ, Best BD, Mannocci L, Fujioka E, Halpin PN, Palka DL, Garrison LP, Mullin KD, Cole TVN, Khan CB, McLellan WM, Pabst DA, Lockhart GG (2015) Density Model for Bryde's Whale (*Balaenoptera edeni*) for the U.S. Gulf of Mexico Version 3.1, 2015-11-06, and Supplementary Report. Marine Geospatial Ecology Lab, Duke University, Durham, North Carolina.

Copyright and License

Revision History

Version	Date	Description of changes
1	2015-01-07	Initial version.
2	2015-01-07	Added four ambiguous "Balaenoptera spp." sightings to the model, following Maze-Foley and Mullin (2006).
2.1	2015-02-02	Updated the documentation, which is still not complete. No changes to the model.
2.2	2015-05-14	Updated calculation of CVs. Switched density rasters to logarithmic breaks. No changes to the model.
3	2015-10-01	At request of L. Garrison and K. Mullin, changed modeling period from 1992-2009 to 1994-2009, so that two sightings of "Bryde's or sei whale" in the western Gulf are not included, under the assumption that Bryde's whales no longer occupy the western Gulf. Added bivariate smooth of XY to the model, to concentrate density where sightings were reported.
3.1	2015-11-06	Small change to the documentation. No changes to the model.

*For questions, or to offer feedback about this model or report, please contact Jason Roberts (jason.roberts@duke.edu)

Survey Data

This analysis only considered effort segments and sightings where year_ >= 1994.

Survey	Period	Length (1000 km)	Hours	Sightings
SEFSC GOMEX92-96 Aerial Surveys	1994-1996	14	78	0
SEFSC Gulf of Mexico Shipboard Surveys, 2003-2009	2003-2009	19	1156	6
SEFSC GulfCet I Aerial Surveys	1994-1994	13	67	0
SEFSC GulfCet II Aerial Surveys	1996-1998	22	124	3
SEFSC GulfSCAT 2007 Aerial Surveys	2007-2007	18	95	2
SEFSC Oceanic CetShip Surveys	1994-2001	32	2078	10
SEFSC Shelf CetShip Surveys	1994-2001	10	707	1
Total		128	4305	22

Table 2: Survey effort and sightings used in this model. Effort is tallied as the cumulative length of on-effort transects and hours the survey team was on effort. Sightings are the number of on-effort encounters of the modeled species for which a perpendicular sighting distance (PSD) was available. Off effort sightings and those without PSDs were omitted from the analysis.

Period	Length (1000 km)	Hours	Sightings
1994-2009	128	4304	22
1998-2009	62	2679	14
% Lost	52	38	36

Table 3: Survey effort and on-effort sightings having perpendicular sighting distances. % Lost shows the percentage of effort or sightings lost by restricting the analysis to surveys performed in 1998 and later, the era in which remotely-sensed chlorophyll and derived productivity estimates are available. See Figure 1 for more information.

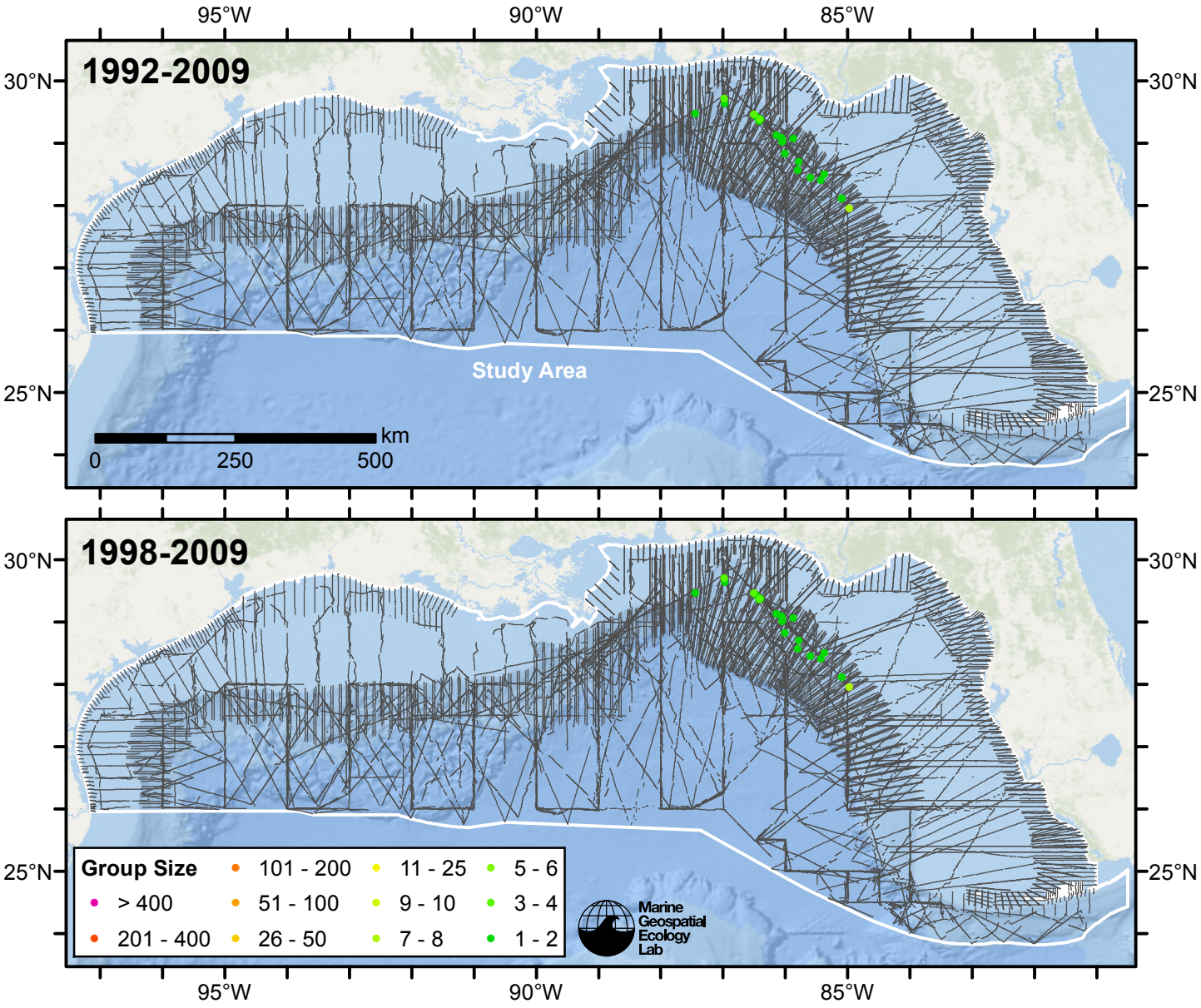

Figure 1: Bryde's whale sightings and survey tracklines. The top map shows all surveys. The bottom map shows surveys performed in 1998 or later. the era in which remotely-sensed chlorophyll and derived productivity estimates are available. Models fitted to contemporaneous (day-of-sighting) estimates of those predictors only utilize these surveys. These maps illustrate the survey data lost in order to utilize those predictors. Models fitted to climatogical estimates of those predictors do not suffer this data loss.

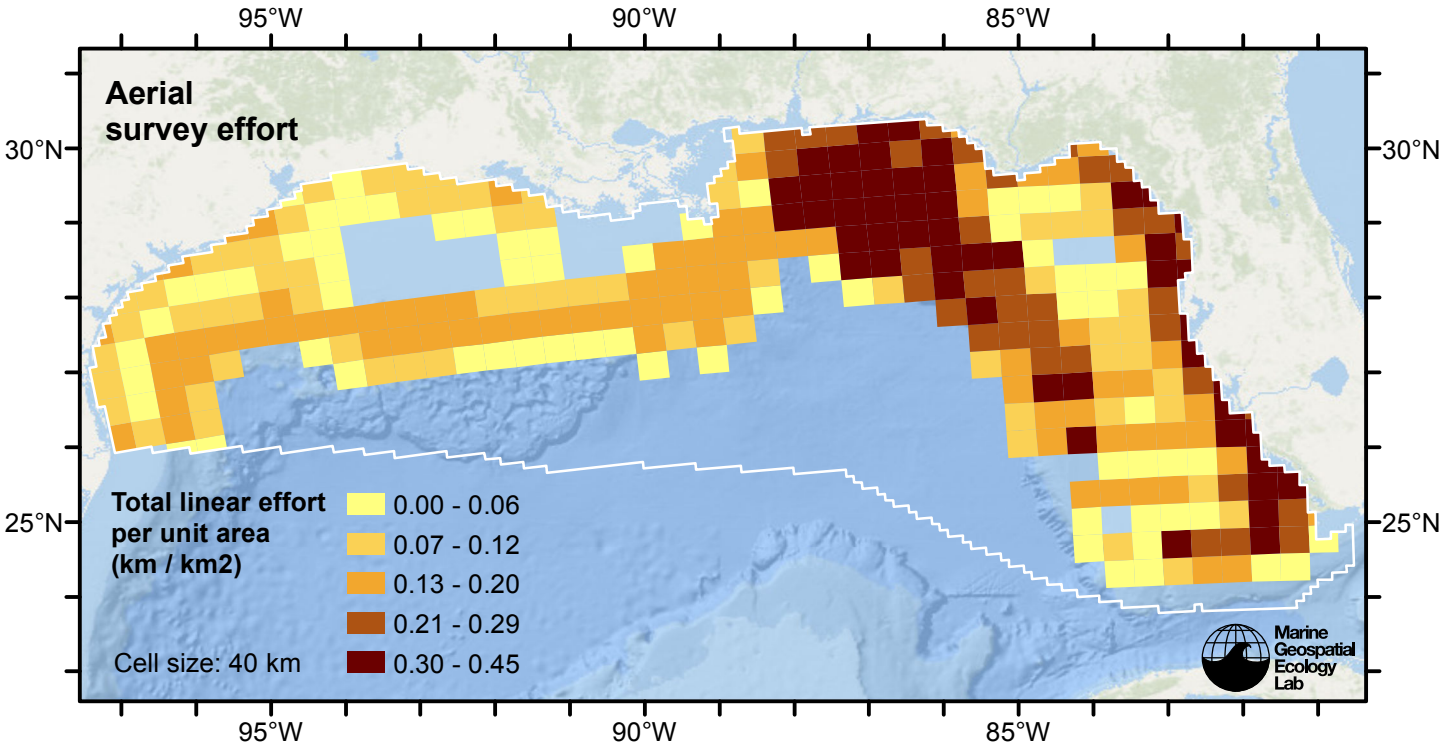

Figure 2: Aerial linear survey effort per unit area.

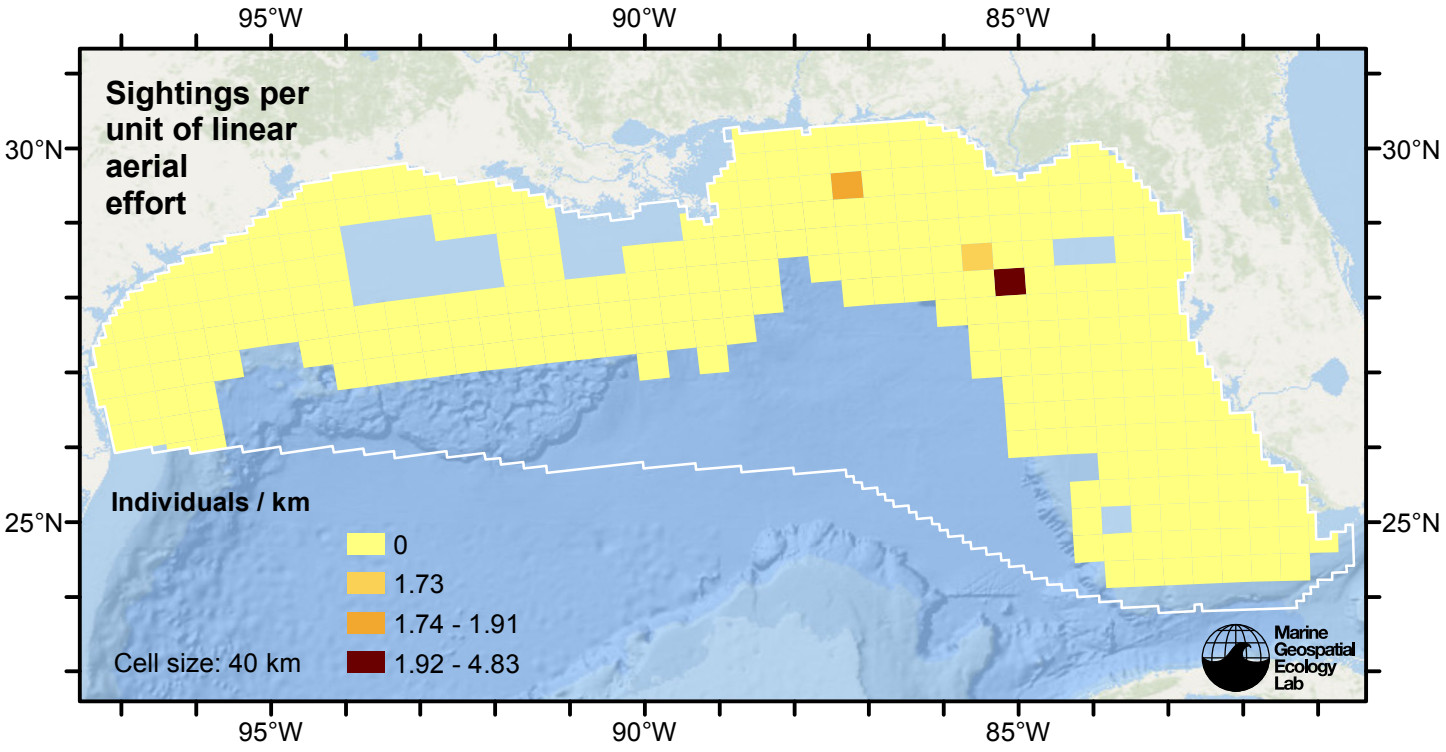

Figure 3: Bryde's whale sightings per unit aerial linear survey effort.

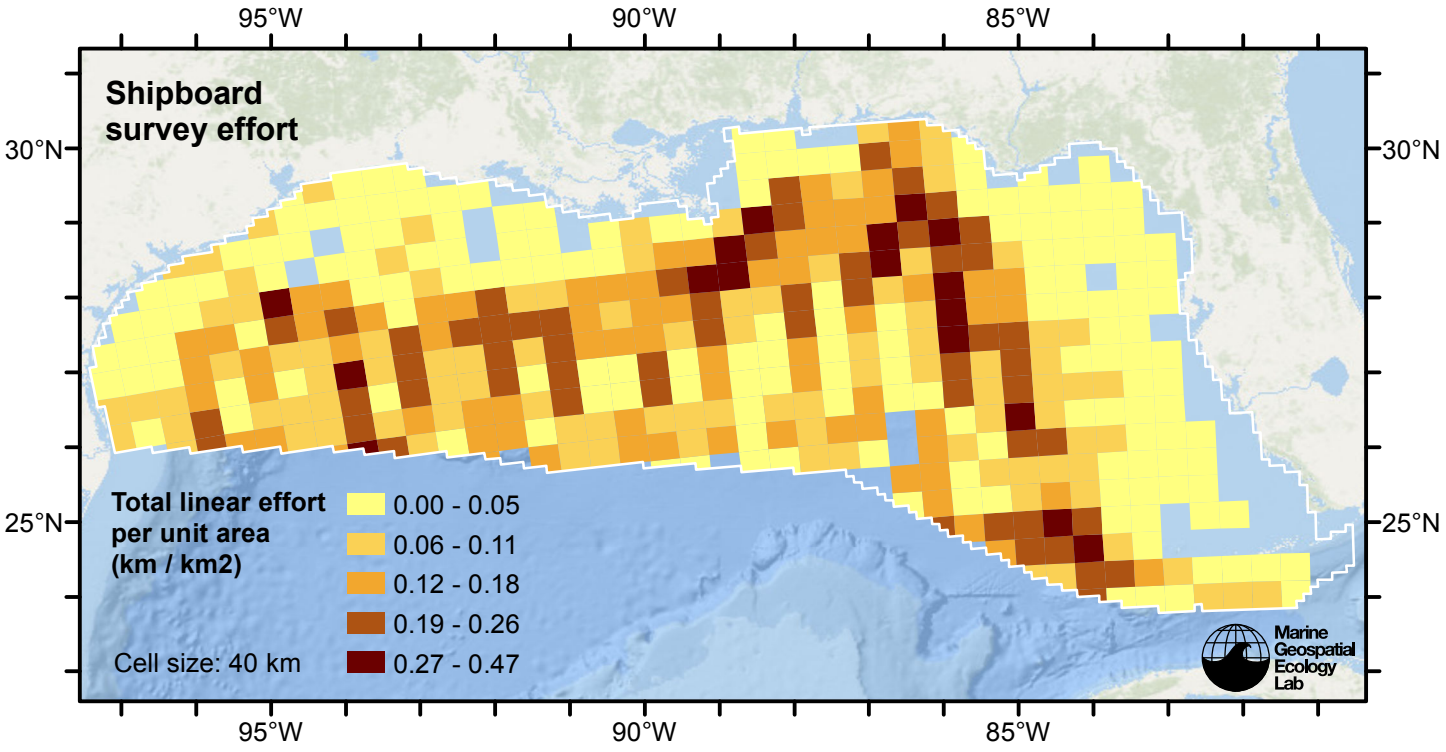

Figure 4: Shipboard linear survey effort per unit area.

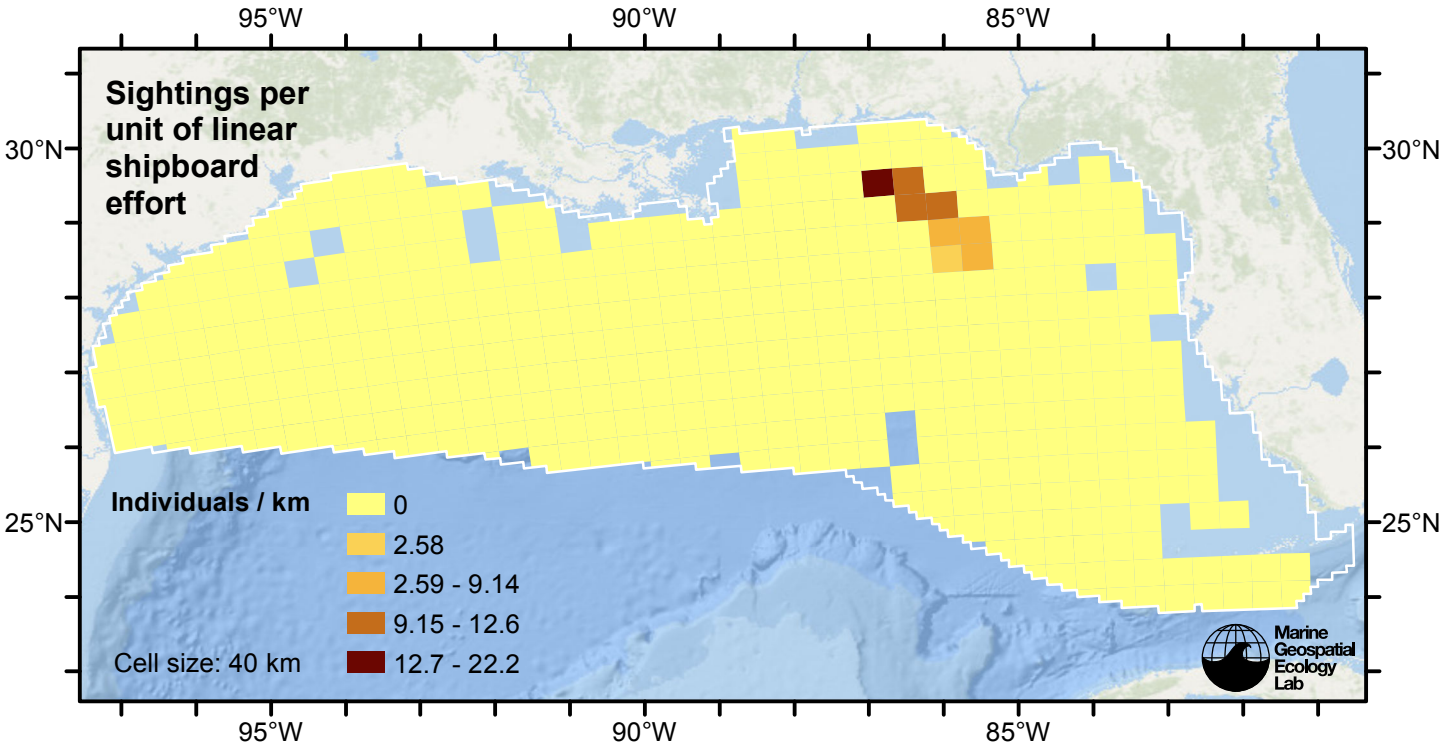

Figure 5: Bryde's whale sightings per unit shipboard linear survey effort.

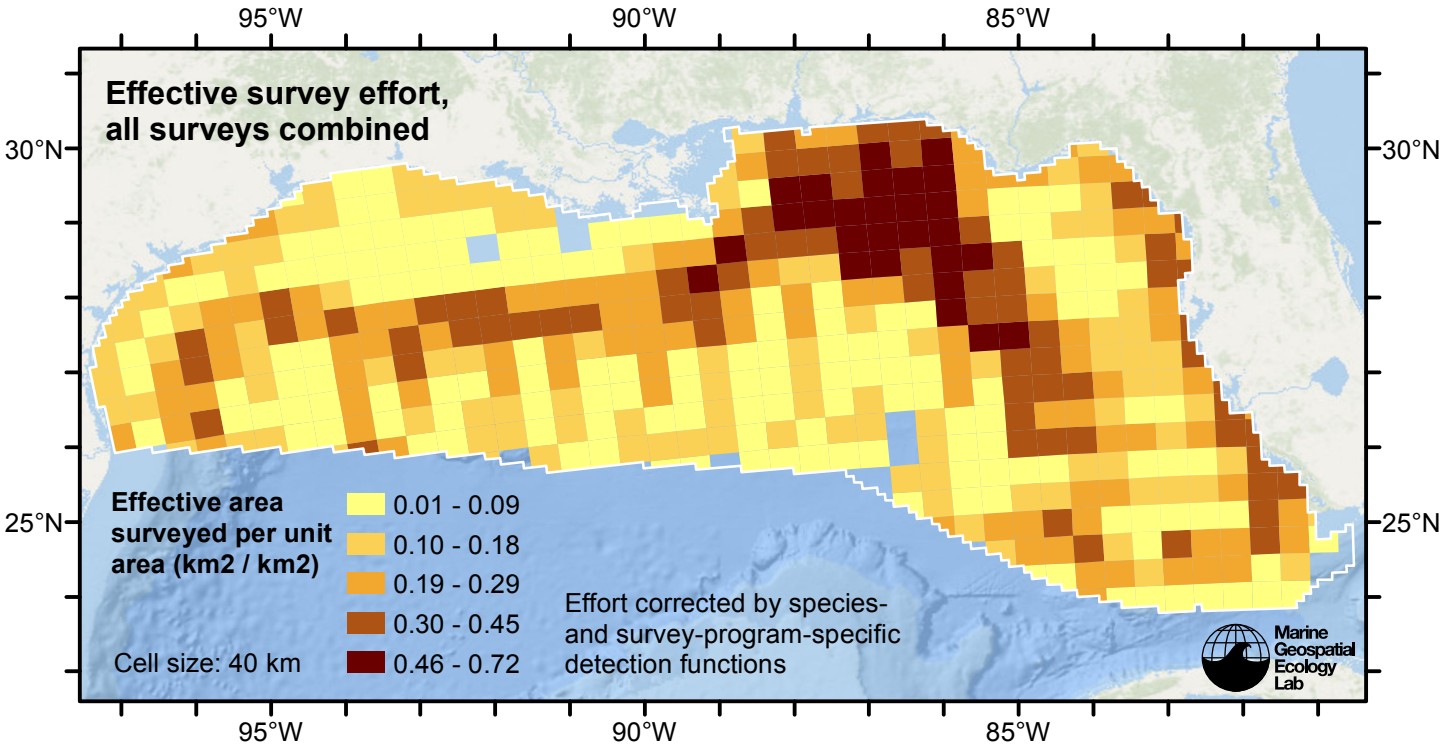

Figure 6: Effective survey effort per unit area, for all surveys combined. Here, effort is corrected by the species- and survey-program-specific detection functions used in fitting the density models.

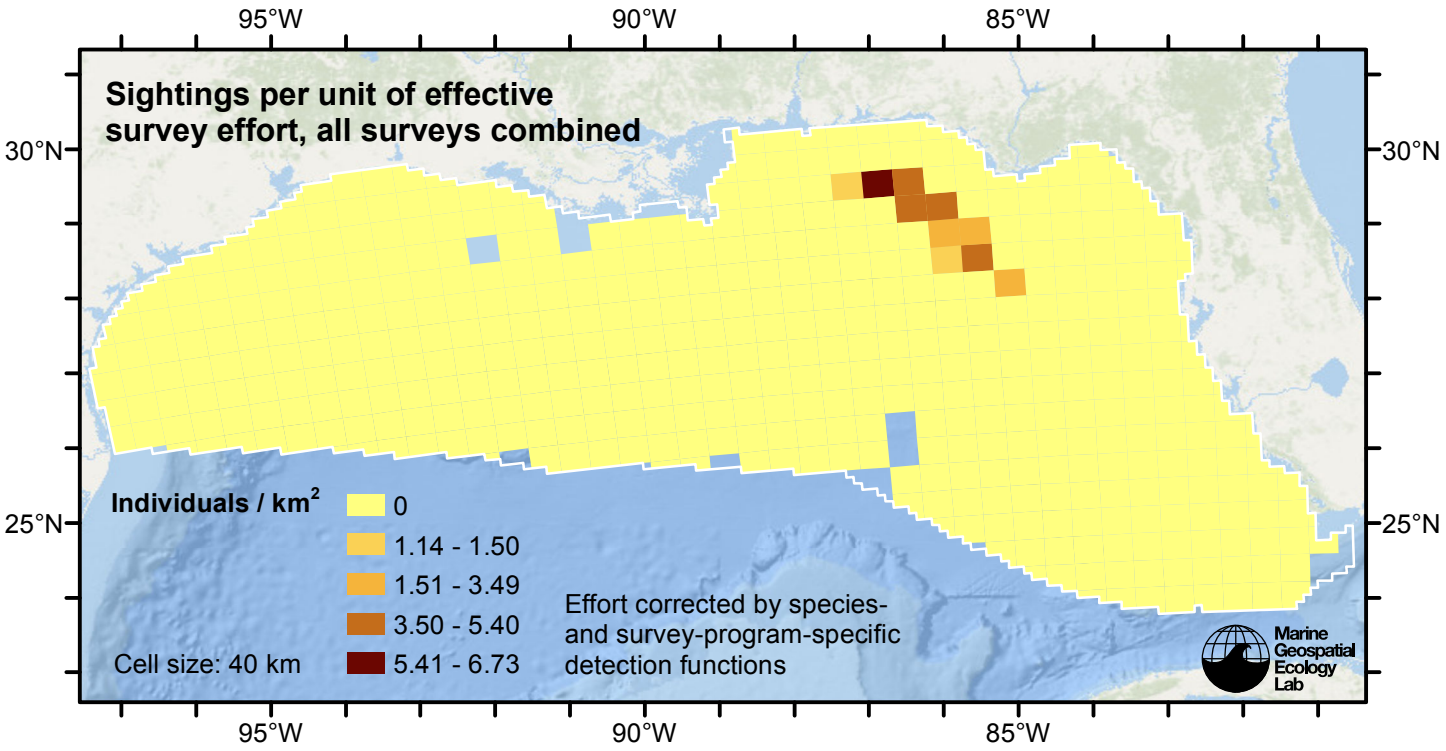

Figure 7: Bryde's whale sightings per unit of effective survey effort, for all surveys combined. Here, effort is corrected by the species- and survey-program-specific detection functions used in fitting the density models.

Detection Functions

The detection hierarchy figures below show how sightings from multiple surveys were pooled to try to achieve Buckland et. al's (2001) recommendation that at least 60-80 sightings be used to fit a detection function. Leaf nodes, on the right, usually represent individual surveys, while the hierarchy to the left shows how they have been grouped according to how similar we believed the surveys were to each other in their detection performance.

At each node, the red or green number indicates the total number of sightings below that node in the hierarchy, and is colored green if 70 or more sightings were available, and red otherwise. If a grouping node has zero sightings–i.e. all of the surveys within it had zero sightings–it may be collapsed and shown as a leaf to save space.

Each histogram in the figure indicates a node where a detection function was fitted. The actual detection functions do not appear in this figure; they are presented in subsequent sections. The histogram shows the frequency of sightings by perpendicular sighting distance for all surveys contained by that node. Each survey (leaf node) recieves the detection function that is closest to it up the hierarchy. Thus, for common species, sufficient sightings may be available to fit detection functions deep in the hierarchy, with each function applying to only a few surveys, thereby allowing variability in detection performance between surveys to be addressed relatively finely. For rare species, so few sightings may be available that we have to pool many surveys together to try to meet Buckland's recommendation, and fit only a few coarse detection functions high in the hierarchy.

A blue Proxy Species tag indicates that so few sightings were available that, rather than ascend higher in the hierarchy to a point that we would pool grossly-incompatible surveys together, (e.g. shipboard surveys that used big-eye binoculars with those that used only naked eyes) we pooled sightings of similar species together instead. The list of species pooled is given in following sections.

Shipboard Surveys

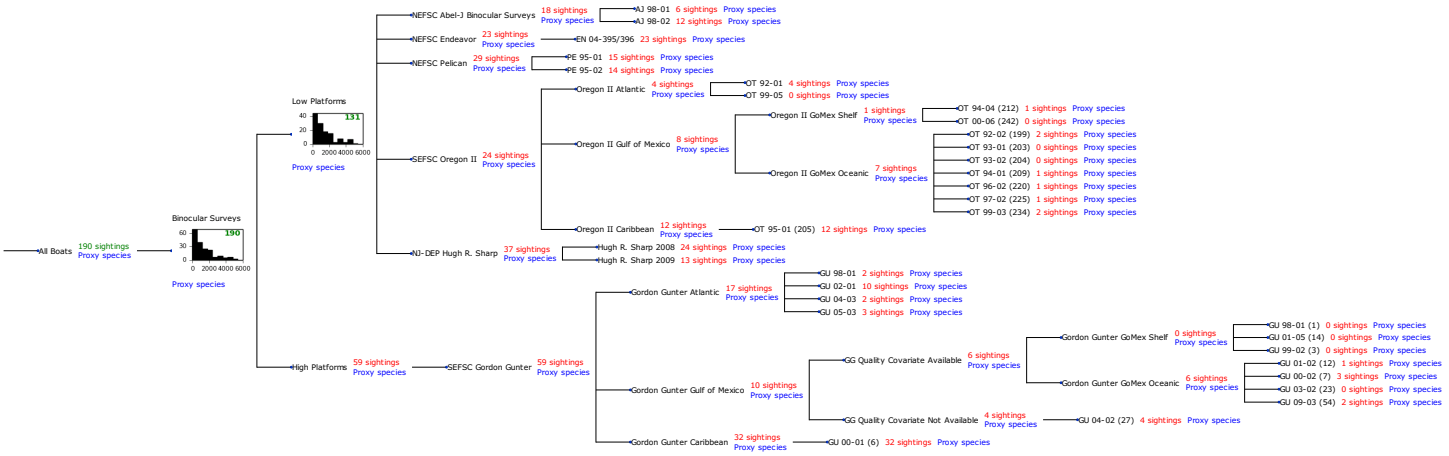

Figure 8: Detection hierarchy for shipboard surveys

Binocular Surveys

Because this taxon was sighted too infrequently to fit a detection function to its sightings alone, we fit a detection function to the pooled sightings of several other species that we believed would exhibit similar detectability. These "proxy species" are listed below.

Reported By Observer	Common Name	n
Balaenoptera	Balaenopterid sp.	7
Balaenoptera acutorostrata	Minke whale	4
Balaenoptera borealis	Sei whale	4
Balaenoptera borealis/edeni	Sei or Bryde's whale	1

Balaenoptera borealis/physalus	Fin or Sei whale	0
Balaenoptera edeni	Bryde's whale	21
Balaenoptera musculus	Blue whale	0
Balaenoptera physalus	Fin whale	98
Eubalaena glacialis	North Atlantic right whale	4
Eubalaena glacialis/Megaptera novaeangliae	Right or humpback whale	0
Megaptera novaeangliae	Humpback whale	46
Total		185

Table 4: Proxy species used to fit detection functions for Binocular Surveys. The number of sightings, n, is before truncation.

The sightings were right truncated at 5500m.

Covariate	Description
beaufort	Beaufort sea state.
size	Estimated size (number of individuals) of the sighted group.
vessel	Vessel from which the observation was made. This covariate allows the detection function to account for vessel-specific biases, such as the height of the survey platform.

Table 5: Covariates tested in candidate "multi-covariate distance sampling" (MCDS) detection functions.

Key	Adjustment	Order	Covariates	Succeeded	Δ AIC	Mean ESHW (m)
hr	poly	2		Yes	0.00	1309
hr	poly	4		Yes	0.47	1353
hr			size	Yes	0.78	1757
hr				Yes	0.80	1542
hn	cos	2		Yes	1.99	1802
hr			beaufort, size	Yes	2.64	1780
hr			beaufort	Yes	2.71	1553
hr			vessel, size	Yes	6.31	1920
hr			vessel	Yes	6.89	1605
hr			beaufort, vessel, size	Yes	8.03	1952
hr			beaufort, vessel	Yes	8.50	1675
hn	cos	3		Yes	9.91	1787
hn			size	Yes	11.86	2317
hn			beaufort, size	Yes	13.68	2319
hn			vessel, size	Yes	15.29	2299
hn			vessel	Yes	17.57	2301

hn				Yes	17.60	2311
hn			beaufort	Yes	19.19	2310
hn	herm	4		No		
hn			beaufort, vessel	No		
hn			beaufort, vessel, size	No		

Table 6: Candidate detection functions for Binocular Surveys. The first one listed was selected for the density model.

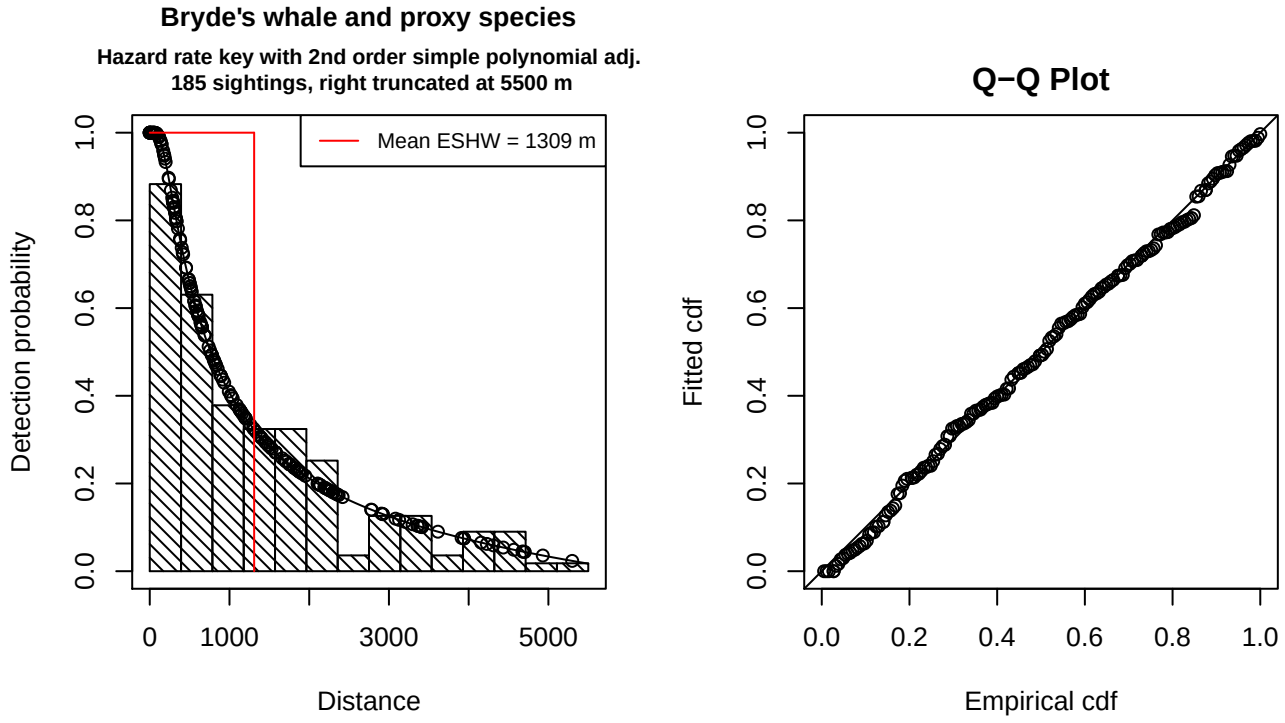

Figure 9: Detection function for Binocular Surveys that was selected for the density model

Statistical output for this detection function:

```
Summary for ds object
Number of observations :  185
Distance range         :  0  -  5500
AIC                    :  3029.944

Detection function:
 Hazard-rate key function with simple polynomial adjustment term of order 2

Detection function parameters
Scale Coefficients:
            estimate        se
(Intercept) 6.295211 0.4058188

Shape parameters:
                estimate        se
(Intercept) 3.297977e-07 0.2305987
```

```
Adjustment term parameter(s):
                estimate        se
poly, order 2 -0.8163338 0.2362958


Monotonicity constraints were enforced.
                     Estimate           SE        CV
Average p            0.238058   0.04195346 0.1762321
N in covered region 777.121568 145.75194793 0.1875536

Monotonicity constraints were enforced.
```

Additional diagnostic plots:

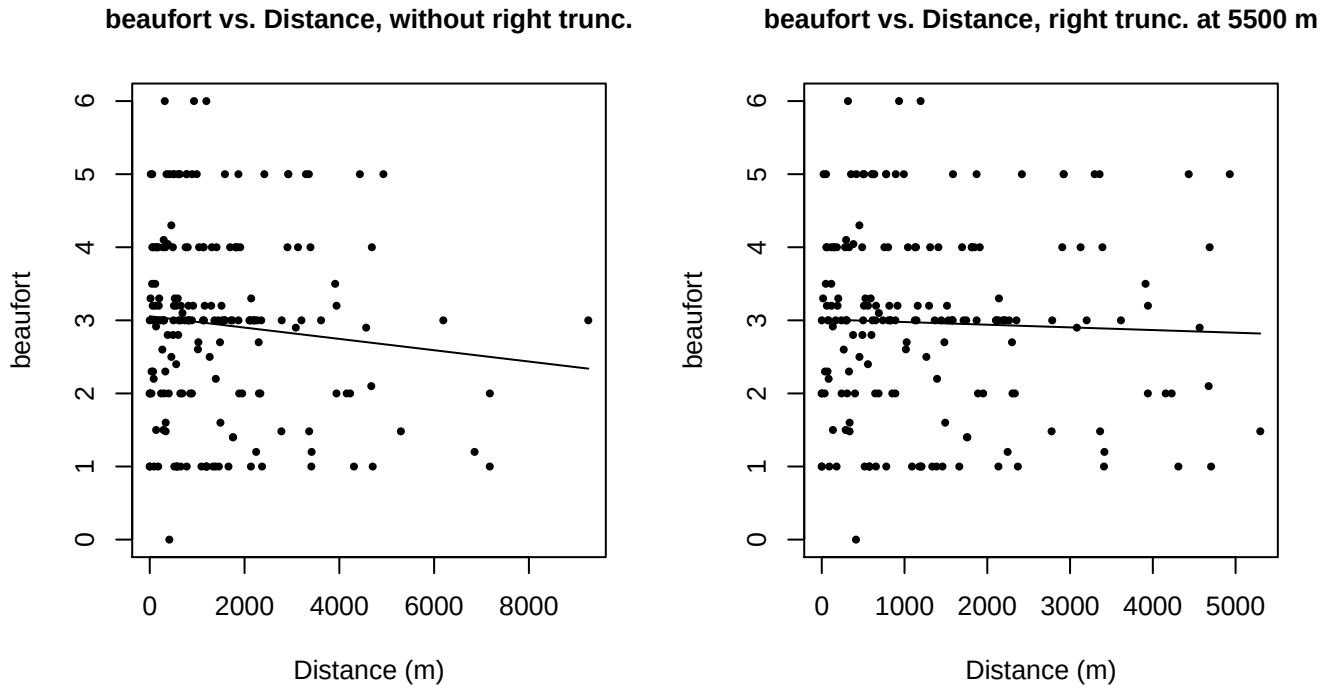

Figure 10: Scatterplots showing the relationship between Beaufort sea state and perpendicular sighting distance, for all sightings (left) and only those not right truncated (right). The line is a simple linear regression.

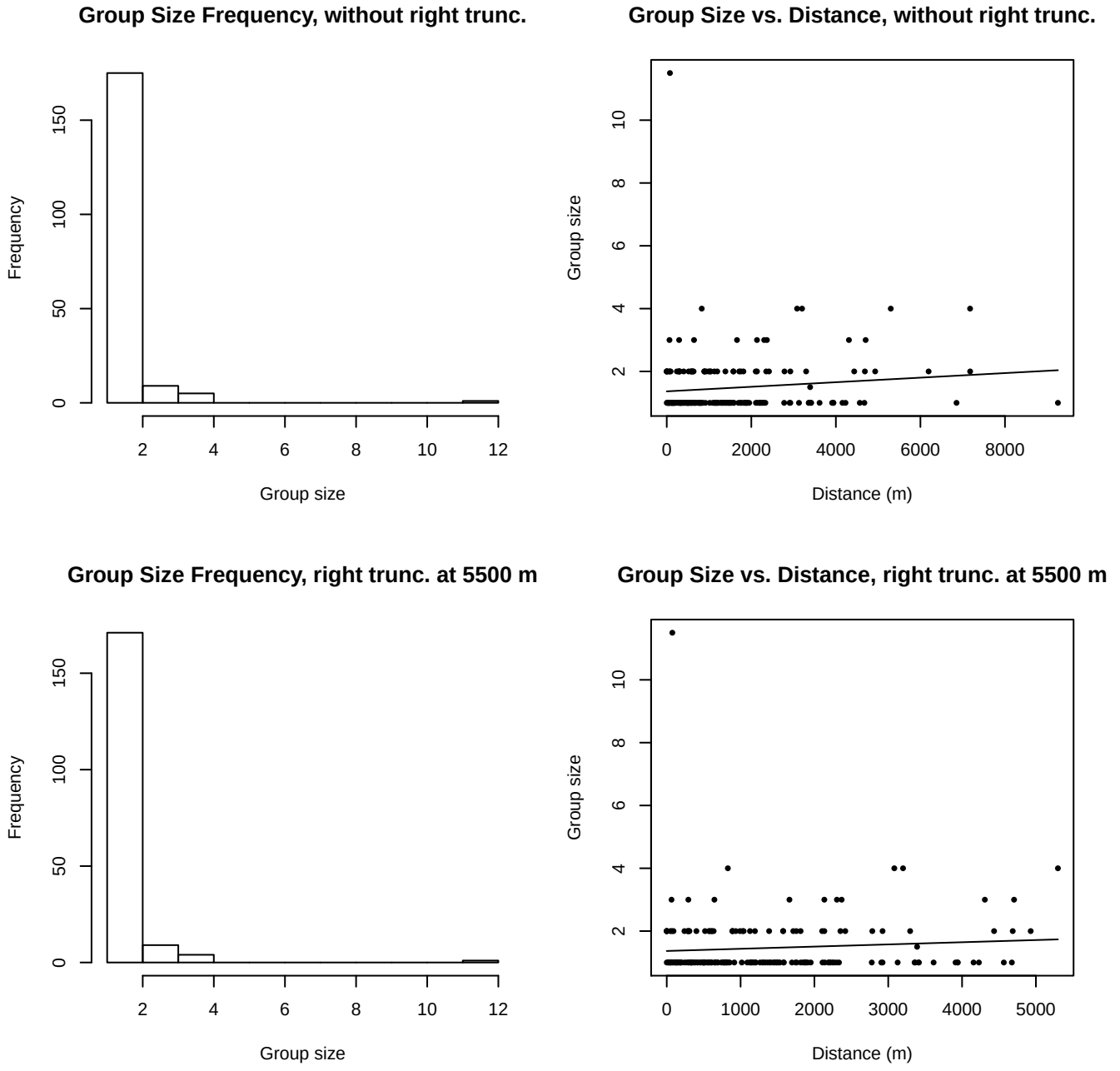

Figure 11: Histograms showing group size frequency and scatterplots showing the relationship between group size and perpendicular sighting distance, for all sightings (top row) and only those not right truncated (bottom row). In the scatterplot, the line is a simple linear regression.

Low Platforms

Because this taxon was sighted too infrequently to fit a detection function to its sightings alone, we fit a detection function to the pooled sightings of several other species that we believed would exhibit similar detectability. These "proxy species" are listed below.

Reported By Observer	Common Name	n
Balaenoptera	Balaenopterid sp.	0
Balaenoptera acutorostrata	Minke whale	3

Balaenoptera borealis	Sei whale	4
Balaenoptera borealis/edeni	Sei or Bryde's whale	0
Balaenoptera borealis/physalus	Fin or Sei whale	0
Balaenoptera edeni	Bryde's whale	7
Balaenoptera musculus	Blue whale	0
Balaenoptera physalus	Fin whale	86
Eubalaena glacialis	North Atlantic right whale	3
Eubalaena glacialis/Megaptera novaeangliae	Right or humpback whale	0
Megaptera novaeangliae	Humpback whale	23
Total		126

Table 7: Proxy species used to fit detection functions for Low Platforms. The number of sightings, n, is before truncation.

The sightings were right truncated at 5500m.

Covariate	Description
beaufort	Beaufort sea state.
size	Estimated size (number of individuals) of the sighted group.
vessel	Vessel from which the observation was made. This covariate allows the detection function to account for vessel-specific biases, such as the height of the survey platform.

Table 8: Covariates tested in candidate "multi-covariate distance sampling" (MCDS) detection functions.

Key	Adjustment	Order	Covariates	Succeeded	Δ AIC	Mean ESHW (m)
hr			size	Yes	0.00	1851
hn	cos	2		Yes	1.87	1764
hr				Yes	1.95	1652
hr			beaufort, size	Yes	1.99	1858
hr			vessel, size	Yes	2.55	2107
hr	poly	4		Yes	3.84	1634
hr	poly	2		Yes	3.89	1634
hr			beaufort, vessel, size	Yes	4.48	2116
hr			vessel	Yes	5.62	1830
hn			size	Yes	6.79	2311
hr			beaufort, vessel	Yes	7.51	1860
hn			vessel, size	Yes	8.30	2288
hn			beaufort, size	Yes	8.64	2312
hn	cos	3		Yes	11.49	1819

hn			vessel	Yes	13.80	2330
hn				Yes	15.66	2345
hn			beaufort	Yes	17.02	2343
hn	herm	4		No		
hr			beaufort	No		
hn			beaufort, vessel	No		
hn			beaufort, vessel, size	No		

Table 9: Candidate detection functions for Low Platforms. The first one listed was selected for the density model.

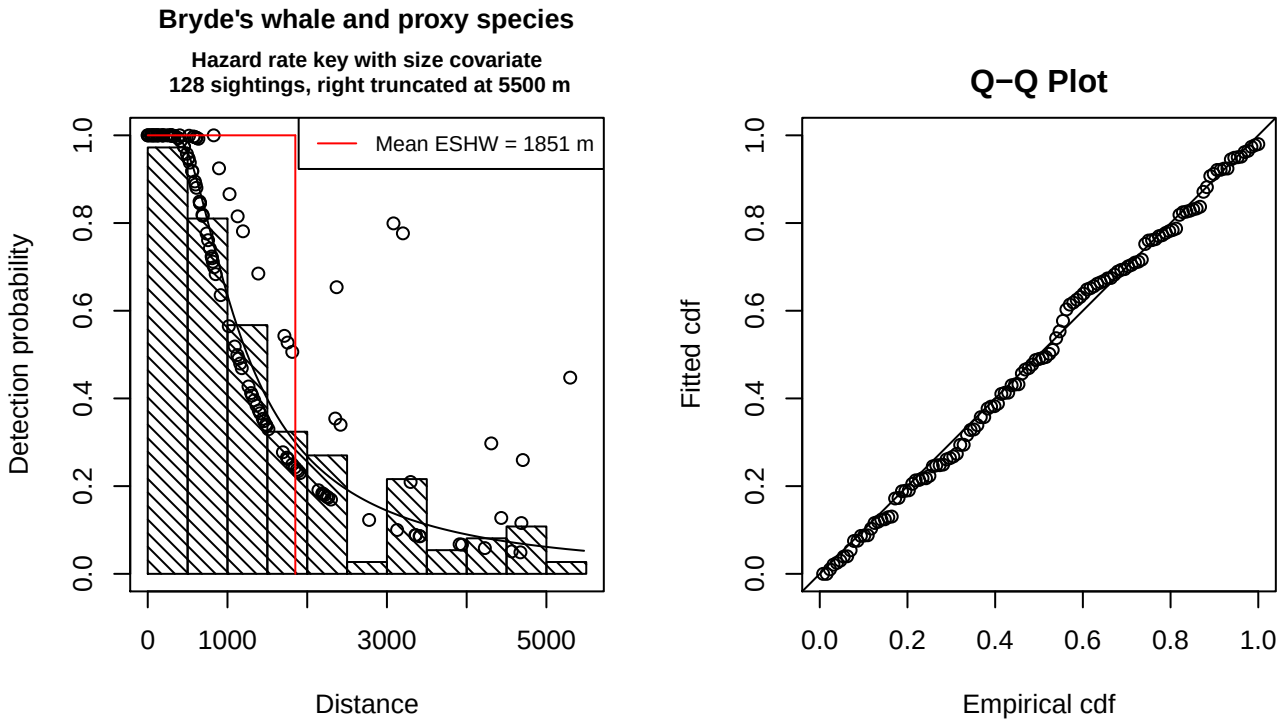

Figure 12: Detection function for Low Platforms that was selected for the density model

Statistical output for this detection function:

```
Summary for ds object
Number of observations :  128
Distance range         :  0  -  5500
AIC                    :  2096.769

Detection function:
 Hazard-rate key function

Detection function parameters
Scale Coefficients:
             estimate        se
(Intercept) 6.3348086 0.3715707
size        0.4890754 0.2062362
```

```
Shape parameters:
             estimate        se
(Intercept) 0.6087008 0.1772532

                       Estimate          SE        CV
Average p             0.3142815  0.03980905 0.1266668
N in covered region 407.2782102 59.82362021 0.1468864
```

Additional diagnostic plots:

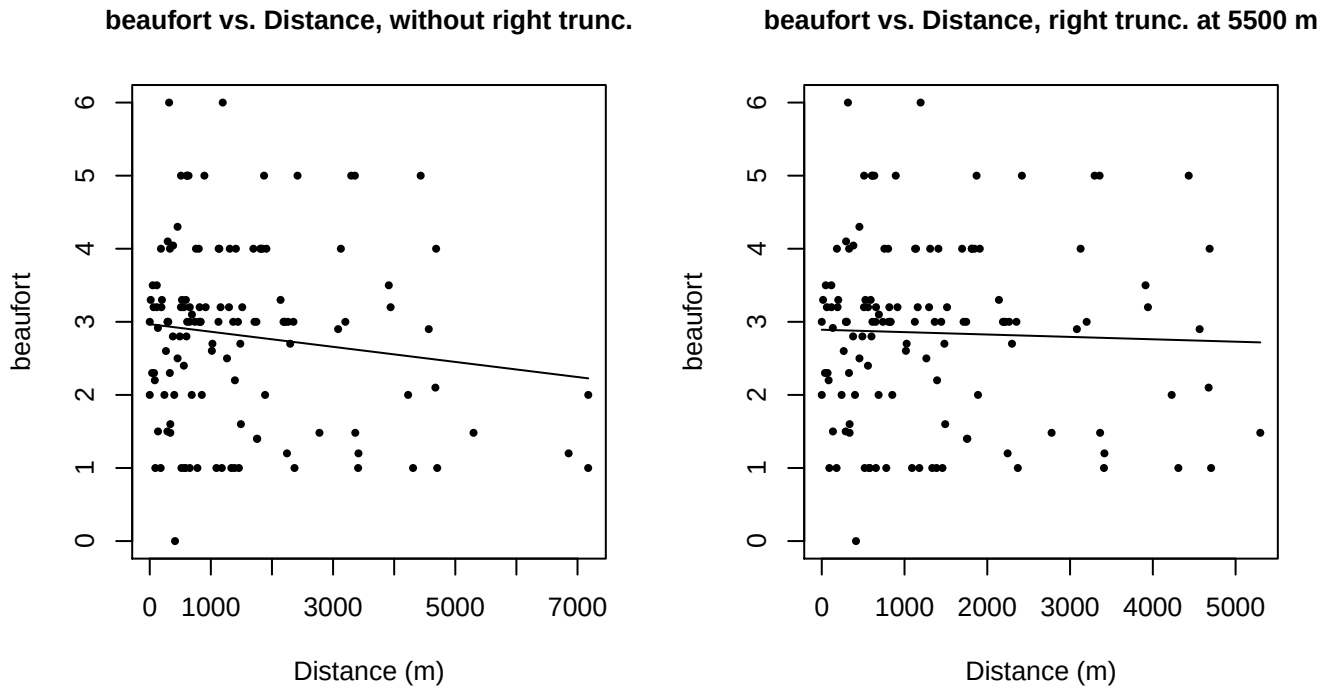

Figure 13: Scatterplots showing the relationship between Beaufort sea state and perpendicular sighting distance, for all sightings (left) and only those not right truncated (right). The line is a simple linear regression.

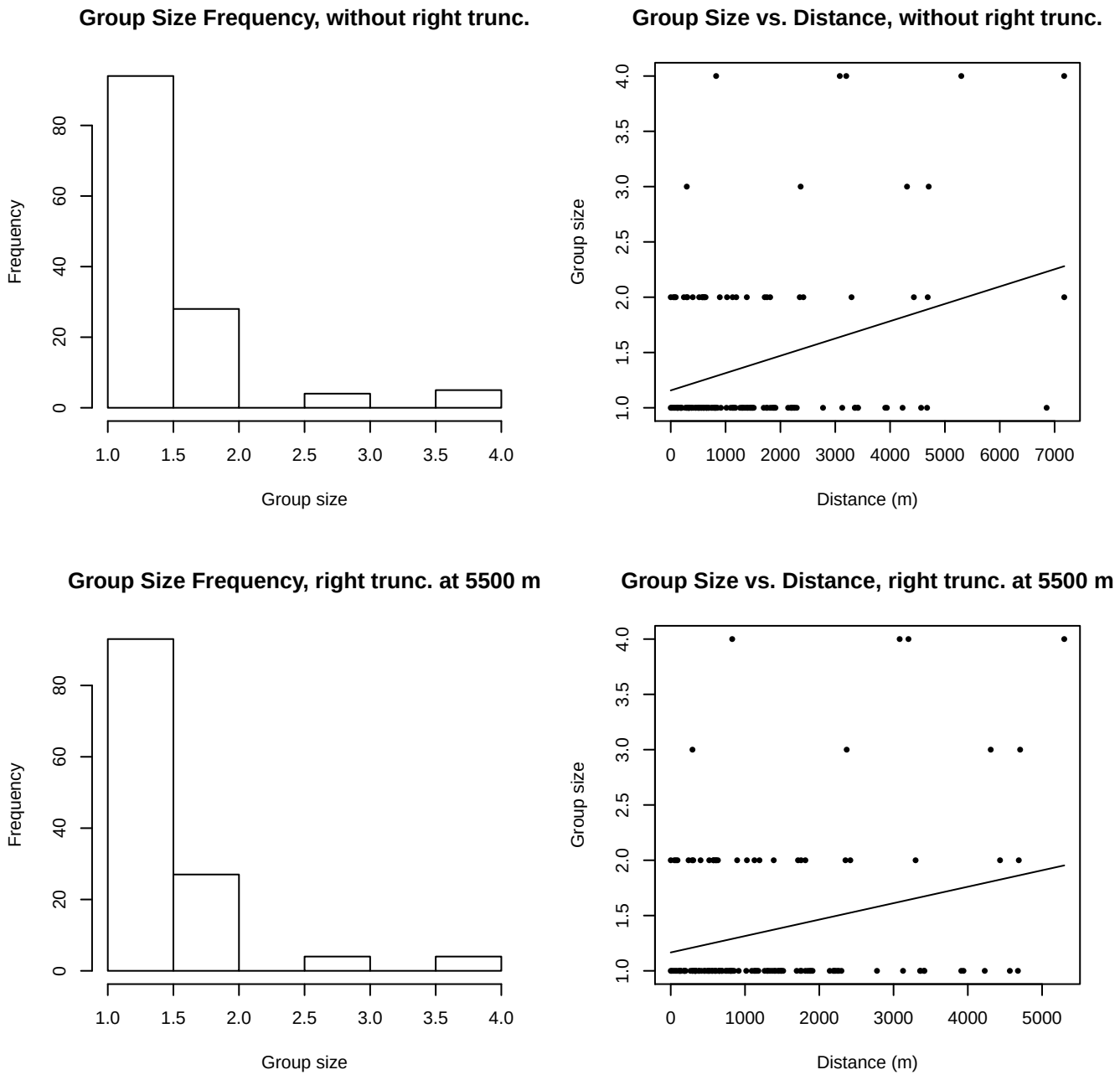

Figure 14: Histograms showing group size frequency and scatterplots showing the relationship between group size and perpendicular sighting distance, for all sightings (top row) and only those not right truncated (bottom row). In the scatterplot, the line is a simple linear regression.

Aerial Surveys

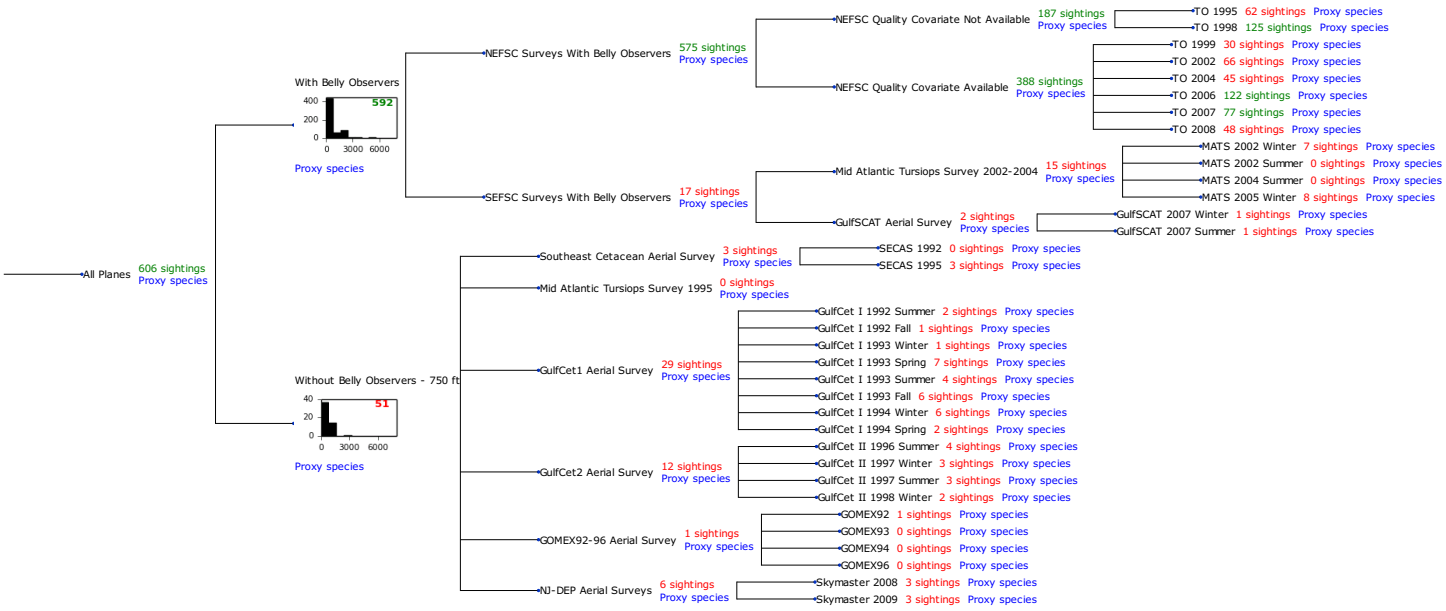

Figure 15: Detection hierarchy for aerial surveys

With Belly Observers

Because this taxon was sighted too infrequently to fit a detection function to its sightings alone, we fit a detection function to the pooled sightings of several other species that we believed would exhibit similar detectability. These "proxy species" are listed below.

Reported By Observer	Common Name	n
Balaenoptera	Balaenopterid sp.	2
Balaenoptera acutorostrata	Minke whale	97
Balaenoptera borealis	Sei whale	14
Balaenoptera borealis/edeni	Sei or Bryde's whale	0
Balaenoptera borealis/physalus	Fin or Sei whale	0
Balaenoptera edeni	Bryde's whale	2
Balaenoptera musculus	Blue whale	1
Balaenoptera physalus	Fin whale	235
Eubalaena glacialis	North Atlantic right whale	43
Eubalaena glacialis/Megaptera novaeangliae	Right or humpback whale	0
Megaptera novaeangliae	Humpback whale	198
Total		592

Table 10: Proxy species used to fit detection functions for With Belly Observers. The number of sightings, n, is before truncation.

The sightings were right truncated at 2000m.

Covariate	Description
beaufort	Beaufort sea state.
size	Estimated size (number of individuals) of the sighted group.

Table 11: Covariates tested in candidate "multi-covariate distance sampling" (MCDS) detection functions.

Key	Adjustment	Order	Covariates	Succeeded	Δ AIC	Mean ESHW (m)
hn	cos	2		Yes	0.00	594
hr	poly	2		Yes	1.71	598
hr	poly	4		Yes	1.86	609
hr			size	Yes	6.10	632
hr				Yes	7.37	627
hn	cos	3		Yes	11.15	585
hn			size	Yes	22.91	705
hn				Yes	23.39	703
hn	herm	4		No		
hn			beaufort	No		
hr			beaufort	No		
hn			beaufort, size	No		
hr			beaufort, size	No		

Table 12: Candidate detection functions for With Belly Observers. The first one listed was selected for the density model.

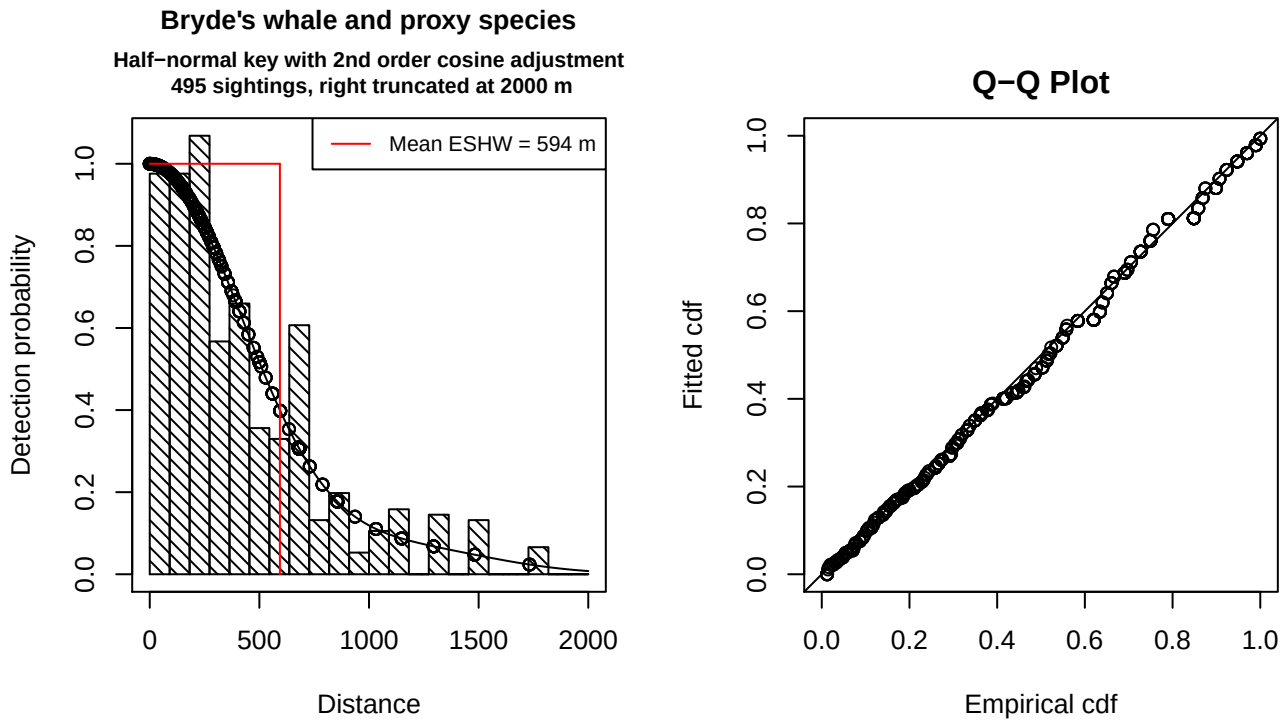

Figure 16: Detection function for With Belly Observers that was selected for the density model

Statistical output for this detection function:

```
Summary for ds object
Number of observations :  495
Distance range         :  0  -  2000
AIC                    :  6960.823

Detection function:
 Half-normal key function with cosine adjustment term of order 2

Detection function parameters
Scale Coefficients:
            estimate         se
(Intercept) 6.464817 0.04316341

Adjustment term parameter(s):
              estimate         se
cos, order 2 0.4286651 0.07975251


Monotonicity constraints were enforced.
                        Estimate          SE         CV
Average p              0.2967565  0.01131844 0.03814048
N in covered region 1668.0342866 89.44444801 0.05362267

Monotonicity constraints were enforced.
```

Additional diagnostic plots:

Figure 17: Scatterplots showing the relationship between Beaufort sea state and perpendicular sighting distance, for all sightings (left) and only those not right truncated (right). The line is a simple linear regression.

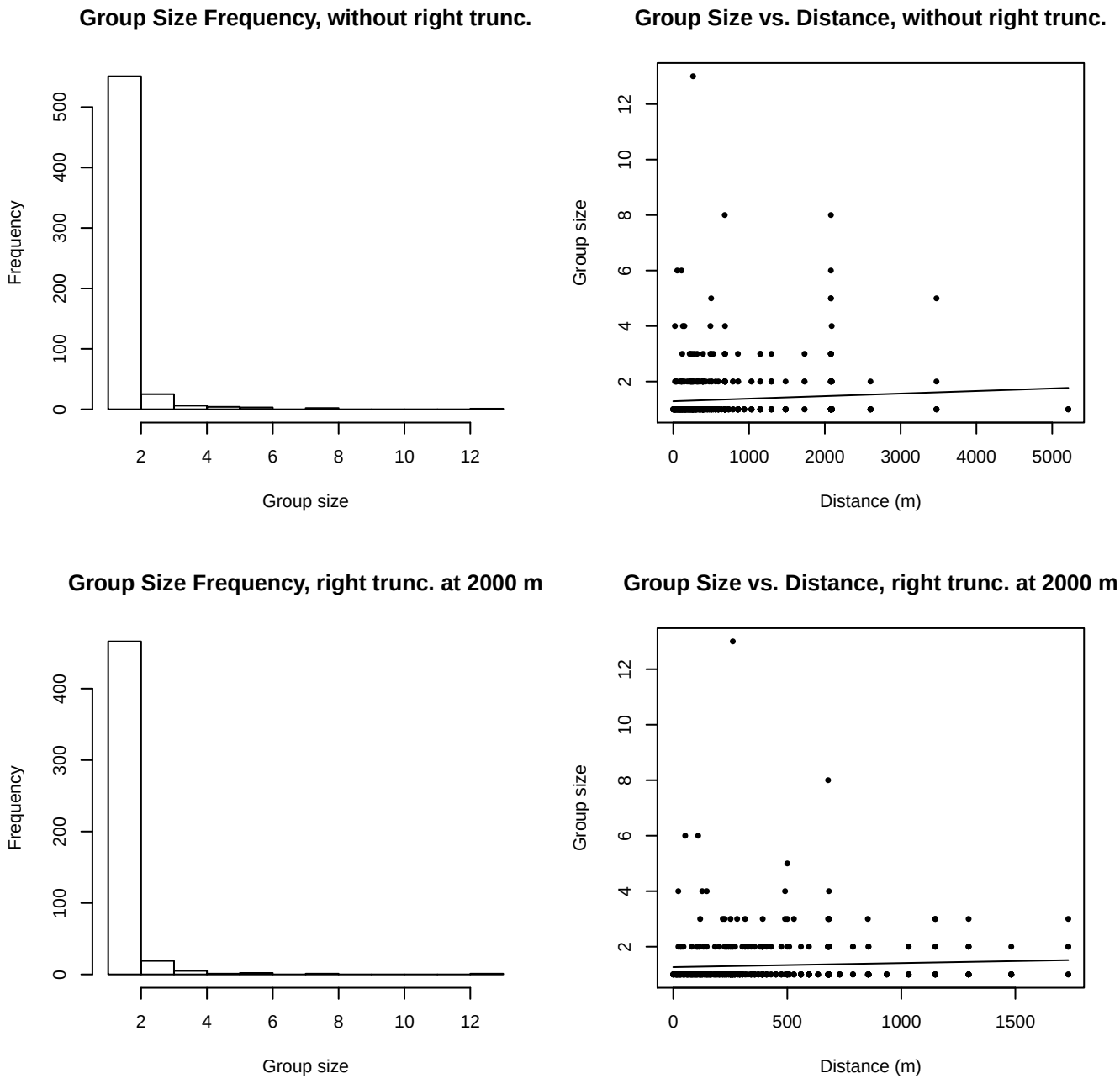

Figure 18: Histograms showing group size frequency and scatterplots showing the relationship between group size and perpendicular sighting distance, for all sightings (top row) and only those not right truncated (bottom row). In the scatterplot, the line is a simple linear regression.

Without Belly Observers - 750 ft

Because this taxon was sighted too infrequently to fit a detection function to its sightings alone, we fit a detection function to the pooled sightings of several other species that we believed would exhibit similar detectability. These "proxy species" are listed below.

Reported By Observer	Common Name	n
Balaenoptera	Balaenopterid sp.	1
Balaenoptera acutorostrata	Minke whale	0

Balaenoptera borealis	Sei whale	0
Balaenoptera borealis/edeni	Sei or Bryde's whale	1
Balaenoptera borealis/physalus	Fin or Sei whale	0
Balaenoptera edeni	Bryde's whale	3
Balaenoptera musculus	Blue whale	0
Balaenoptera physalus	Fin whale	1
Eubalaena glacialis	North Atlantic right whale	0
Eubalaena glacialis/Megaptera novaeangliae	Right or humpback whale	0
Megaptera novaeangliae	Humpback whale	6
Physeter macrocephalus	Sperm whale	17
Total		29

Table 13: Proxy species used to fit detection functions for Without Belly Observers - 750 ft. The number of sightings, n, is before truncation.

The sightings were right truncated at 600m. Due to a reduced frequency of sightings close to the trackline that plausibly resulted from the behavior of the observers and/or the configuration of the survey platform, the sightings were left truncted as well. Sightings closer than 40 m to the trackline were omitted from the analysis, and it was assumed that the the area closer to the trackline than this was not surveyed. This distance was estimated by inspecting histograms of perpendicular sighting distances. The vertical sighting angles were heaped at 10 degree increments, so the candidate detection functions were fitted using linear bins scaled accordingly.

Key	Adjustment	Order	Covariates	Succeeded	Δ AIC	Mean ESHW (m)
hn	cos	2		Yes	0.00	216
hr				Yes	0.59	251
hn	cos	3		Yes	2.31	255
hn	herm	4		Yes	2.46	316
hr	poly	2		Yes	2.59	251
hr	poly	4		Yes	2.63	244
hn				No		

Table 14: Candidate detection functions for Without Belly Observers - 750 ft. The first one listed was selected for the density model.

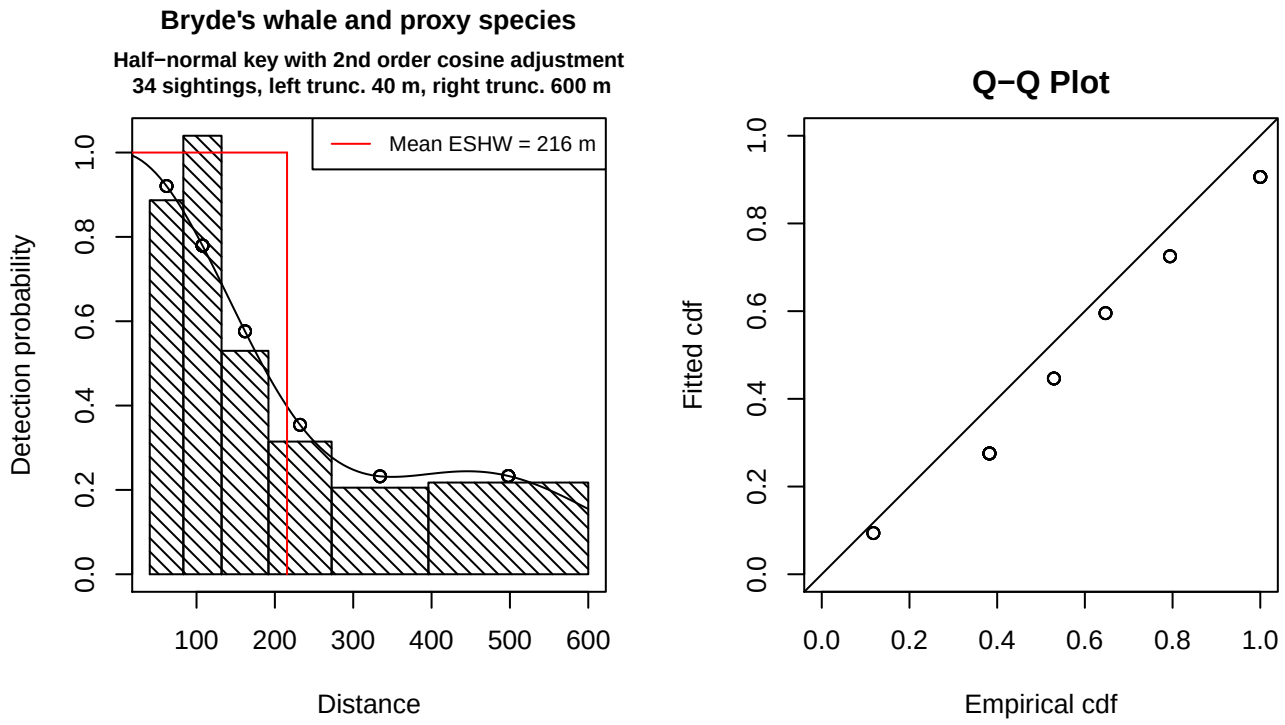

Figure 19: Detection function for Without Belly Observers - 750 ft that was selected for the density model

Statistical output for this detection function:

```
Summary for ds object
Number of observations :  34
Distance range         :  40.30835  -  600
AIC                    :  124.984

Detection function:
 Half-normal key function with cosine adjustment term of order 2

Detection function parameters
Scale Coefficients:
            estimate        se
(Intercept) 5.738324 0.1838281

Adjustment term parameter(s):
              estimate       se
cos, order 2 0.4333816 0.242253


Monotonicity constraints were enforced.
                     Estimate         SE        CV
Average p            0.3592782  0.0870934 0.2424122
N in covered region 94.6341976 26.3634680 0.2785829

Monotonicity constraints were enforced.
```

Additional diagnostic plots:

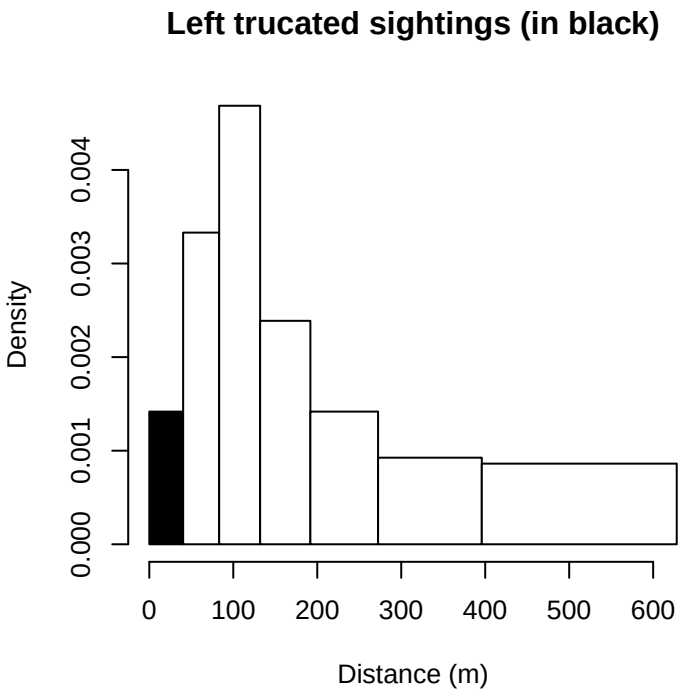

Figure 20: Density of sightings by perpendicular distance for Without Belly Observers - 750 ft. Black bars on the left show sightings that were left truncated.

g(0) Estimates

Platform	Surveys	Group Size	*g(0)*	Biases Addressed	Source
Shipboard	All	Any	0.90	Perception	Barlow (2006)
Aerial	All	1-5	0.53	Both	Palka (2006)
		>5	1.00	Both	Palka (2006)

Table 15: Estimates of *g(0)* used in this density model.

No species- or survey-specific estimates of g(0) were available for Bryde's whales for any surveys in our study. For shipboard surveys, we used Barlow's (2006) estimate (0.90), produced from several years of dual-team surveys in the Pacific ocean that used similar binoculars and protocols to the binocular surveys in our study. The estimate accounted for perception bias but not availability bias.

For aerial surveys, for small groups, defined here as 1-5 individuals, we used Palka's (2006) estimate of g(0) for groups of 1-5 large whales, estimated from two years of aerial surveys using the Hiby (1999) circle-back method. This estimate accounted for both availability and perception bias, but pooled sightings of several species together to provide a generic estimate for all large whales, due to sample-size limitations. For large groups, defined as greater than 5 individuals, Palka (2006) assumed that g(0) was 1.

Density Model

Bryde's whales have a circumtropical distribution, generally inhabit waters of 16 C or warmer, do not move poleward of 40 N, and are found both offshore and near the coast in many areas (Jefferson et al. 2008). All of the baleen whales except Bryde's whale appear to be extralimital in the Gulf of Mexico (Jefferson and Schiro 1997). A recent genetic analysis concluded that the genetic divergence of the Gulf of Mexico population from other Bryde's whale populations is large enough that it may warrant elevation of this genotype to a separate species or subspecies (Rosel and Wilcox 2014).

The surveys used in our study, spanning 1992-2009, reported 17 definitive sightings of Bryde's whales, all between the 180 and 270 m isobaths, near to and southeast of the DeSoto Canyon, along the continental slope of the northeastern Gulf of Mexico. These sightings spanned multiple years (1996, 1997, 1999, 2000, 2004, 2007, 2009) and months (February-August). The surveys also reported four ambiguous "Bryde's or sei whale" sightings. Two of these occurred in the same area as the 17 definitive sightings, in April 1992 and May 2001. The other two occurred in the western Gulf, south of western Louisiana near the continental shelf break at roughly 280 and 420 m, in June 1992 and February 1993. Finally, the surveys reported four ambiguous "Balaenoptera spp." sightings, which all occurred near DeSoto Canyon, in the area where the definitive sightings occurred. Following Maze-Foley and Mullin (2006), who believed that the only balaenopterid whale sighted during NOAA's surveys was the Bryde's whale, we considered these 8 ambiguous sightings to be Bryde's whales.

All but two of the 25 sightings occurred along the northeastern slope near DeSoto Canyon. The other two occurred in a similar depth range but in the western Gulf in the first two years of the study period. While these were likely Bryde's whales, no other sightings have been reported west of the Mississippi River in over 20 years. Rosel and Wilcox (2014), summarizing the whaling study of Reeves et al. (2011), noted that whaling records suggest Bryde's whales once had a broader distribution in the Gulf. They pointed out that modern-day energy exploration and production in the Gulf of Mexico peaks in shelf and slope waters west of the Mississippi River Delta, and speculated that habitat disruption, noise, and vessel traffic could have resulted in the abandonment of the northwestern Gulf by Bryde's whales. LaBrecque et al. (2015), who reviewed the work of Rosel and Wilcox (2014) and others, defined a Biologically Important Area (BIA) for Bryde's whales in the northeastern Gulf slope and did not describe the western Gulf as important habitat for Bryde's whales.

Reflecting the lack of definitive sightings beyond the cluster in the northeastern Gulf, the lack of Bryde's whale sightings in the western Gulf during abundance surveys after 1993, and the expert opinion of our NOAA SEFSC coauthors (Garrison and Mullin), we eliminated the first two years of survey data from our Gulf of Mexico Bryde's whale model, constructing it from surveys from 1994-2009, which reported the 23 sightings in the northeastern Gulf.

With this number and spatial distribution of sightings, we faced a dilemma. On the one hand, the limited number of sightings precluded the possibility of fitting a complex multivariate regression and allowing the environmental covariates to flesh out a detailed habitat-based description of Bryde's whale spatial distribution. On the other hand, all of the sightings occurred along the northeastern slope within a narrow depth range, spanning multiple years and seasons. We were reluctant to produce a model that not reflect this, as would occur, for example, with a simple stratified model that assumed Bryde's whales were absent shallower than 100 m and distributed uniformly deeper than 100 m, throughout the entire northern Gulf of Mexico.

To allow the model to concentrate density in the area where sightings occurred while remaining parsimonious as a precaution against overfitting, we fitted a simple model with two static terms: a bivariate smooth of spatial coordinates and the logarithm of depth.

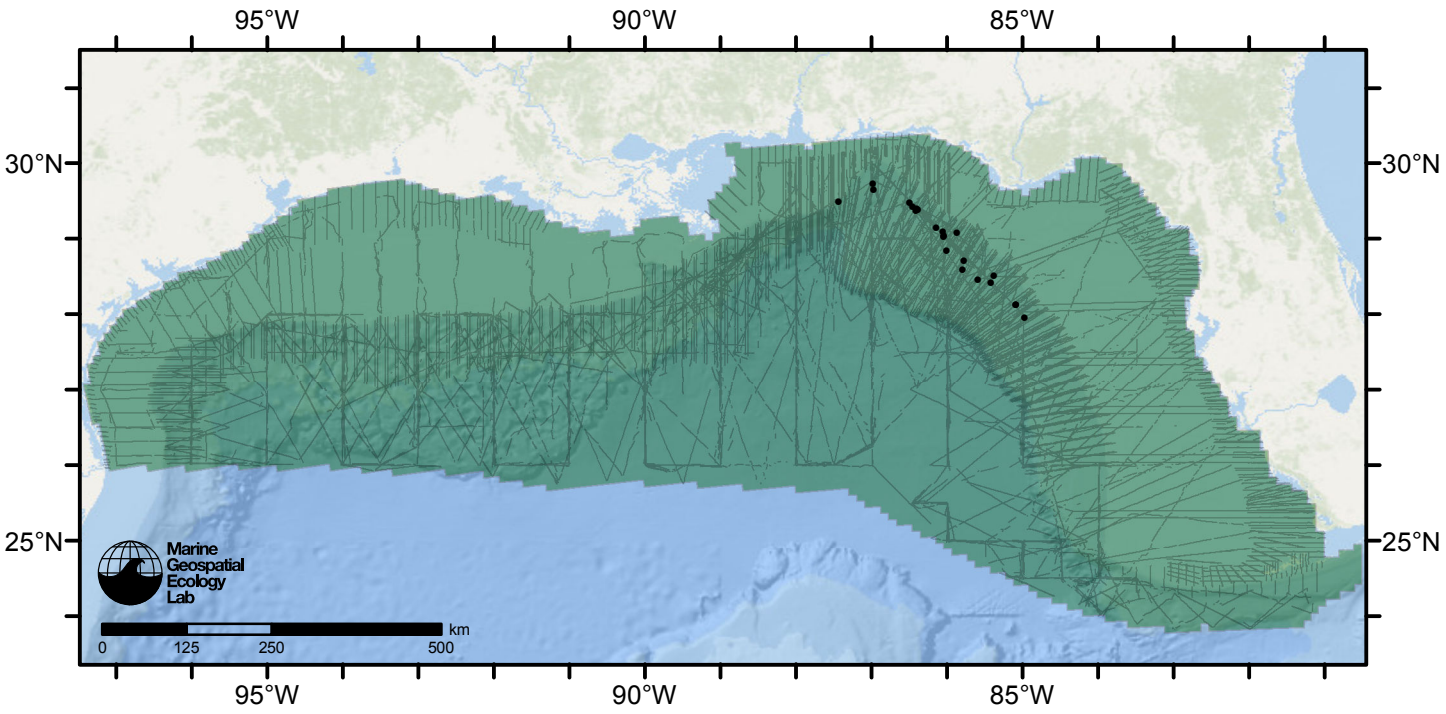

Figure 21: Bryde's whale density model schematic. All on-effort sightings are shown, including those that were truncated when detection functions were fitted.

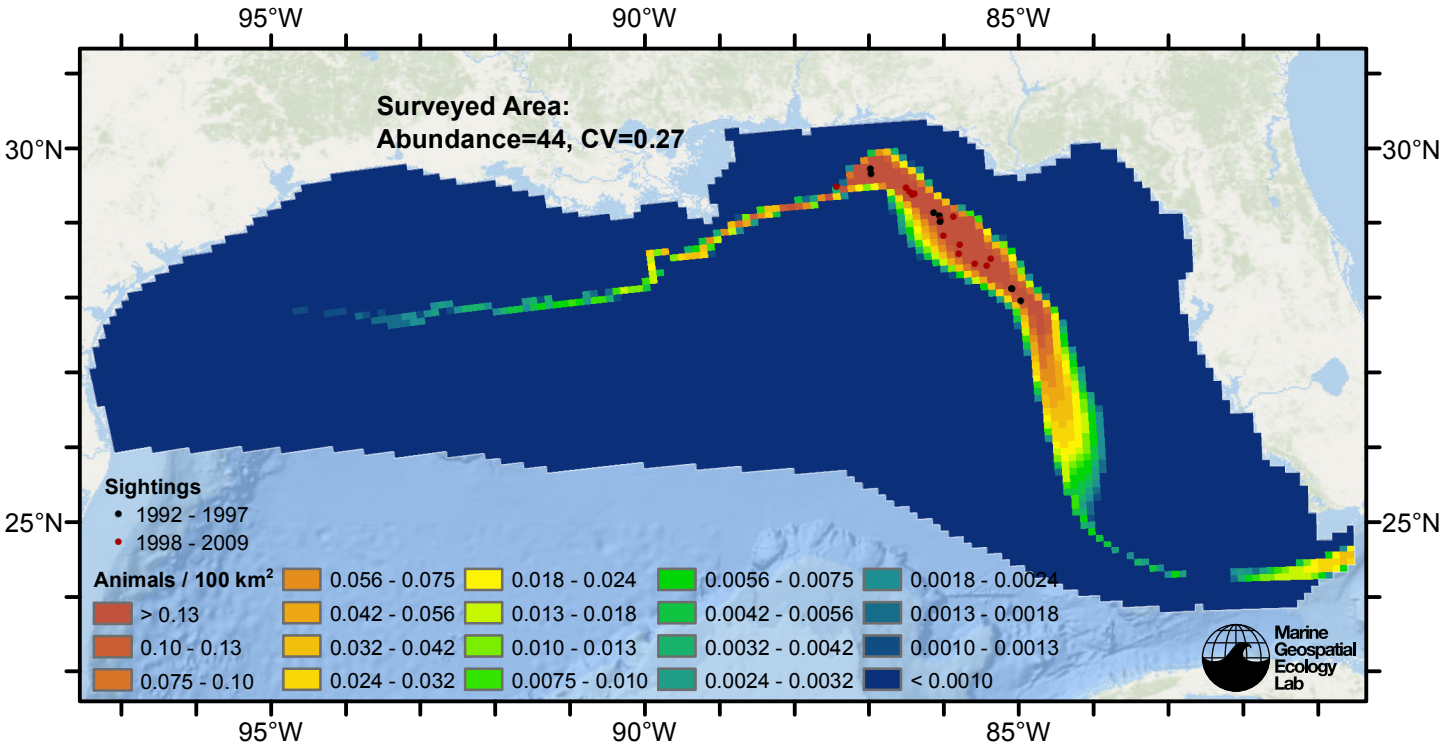

Figure 22: Bryde's whale density predicted by the climatological model that explained the most deviance. Pixels are 10x10 km. The legend gives the estimated individuals per pixel; breaks are logarithmic. Abundance for each region was computed by summing the density cells occuring in that region.

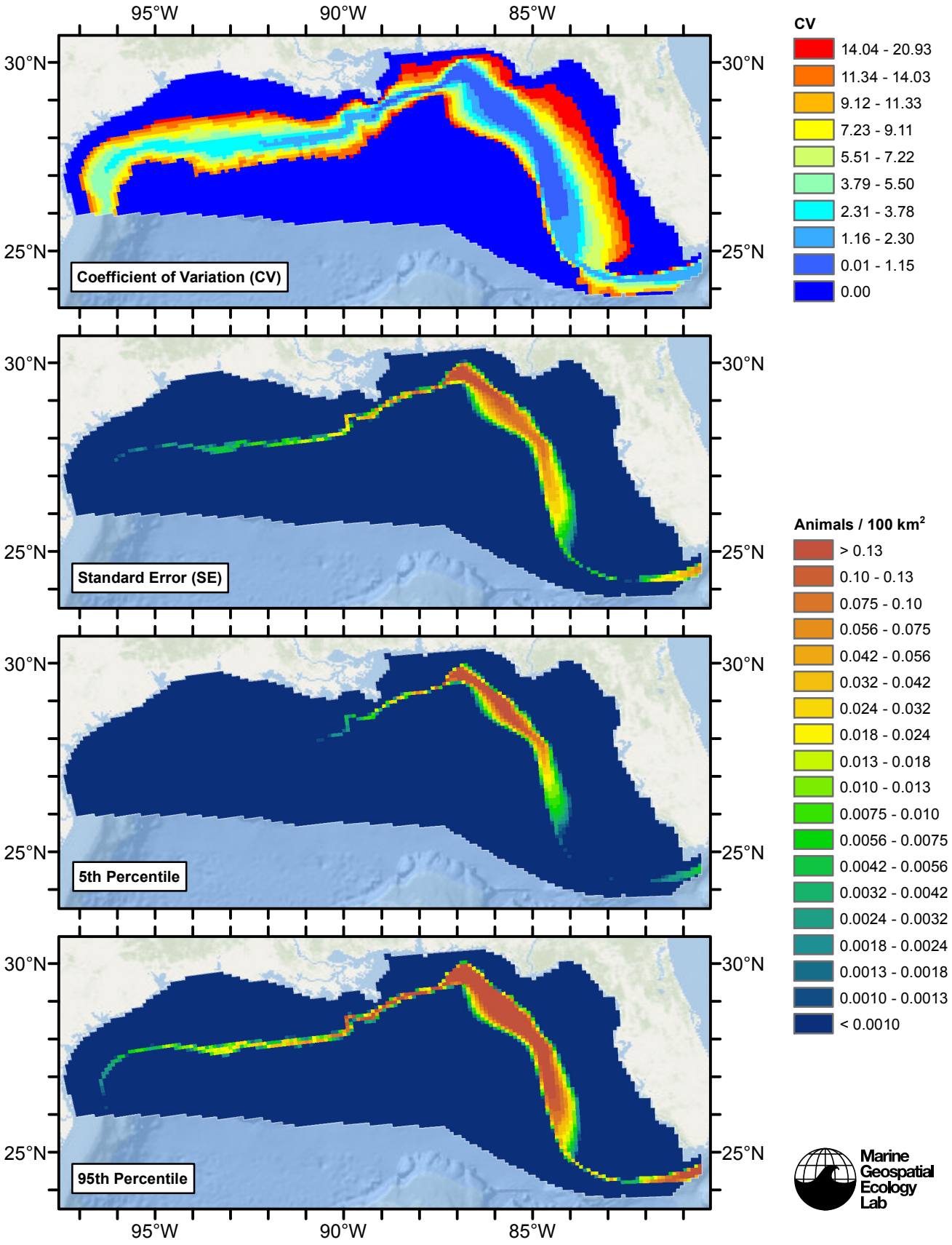

Figure 23: Estimated uncertainty for the climatological model that explained the most deviance. These estimates only incorporate the statistical uncertainty estimated for the spatial model (by the R mgcv package). They do not incorporate uncertainty in the detection functions, g(0) estimates, predictor variables, and so on.

Surveyed Area

Statistical output

```
Rscript.exe: This is mgcv 1.8-4. For overview type 'help("mgcv-package")'.


Family: Tweedie(p=1.159)
Link function: log

Formula:
abundance ~ offset(log(area_km2)) + s(x, y, bs = "ts", k = 60) +
    s(log10(Depth), bs = "ts", k = 5)

Parametric coefficients:
            Estimate Std. Error t value Pr(>|t|)
(Intercept)   -34.55      12.00  -2.879  0.00399 **
---
Signif. codes:  0 '***' 0.001 '**' 0.01 '*' 0.05 '.' 0.1 ' ' 1

Approximate significance of smooth terms:
                  edf Ref.df     F p-value
s(x,y)          1.736     44 0.203 0.00615 **
s(log10(Depth)) 1.907      4 2.099 0.01087 *
---
Signif. codes:  0 '***' 0.001 '**' 0.01 '*' 0.05 '.' 0.1 ' ' 1

R-sq.(adj) =  0.0103   Deviance explained = 50.4%
-REML = 147.78  Scale est. = 12.394    n = 13163

All predictors were significant. This is the final model.
Creating term plots.
Diagnostic output from gam.check():

Method: REML   Optimizer: outer newton
full convergence after 15 iterations.
Gradient range [-7.456951e-08,5.644545e-08]
(score 147.779 & scale 12.39375).
Hessian positive definite, eigenvalue range [0.3751267,128.7345].
Model rank =  64 / 64

Basis dimension (k) checking results. Low p-value (k-index<1) may
indicate that k is too low, especially if edf is close to k'.

                   k'    edf k-index p-value
s(x,y)          59.000  1.736   1.021    0.72
s(log10(Depth))  4.000  1.907   0.956    0.02

Predictors retained during the model selection procedure: Depth

Predictors dropped during the model selection procedure:
```

Model term plots

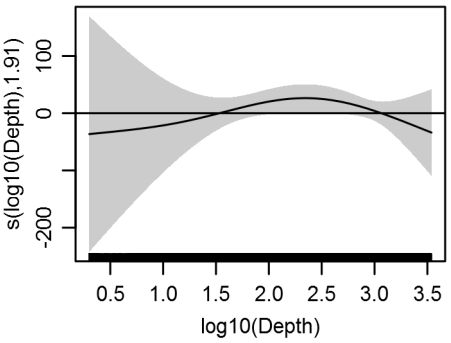

Diagnostic plots

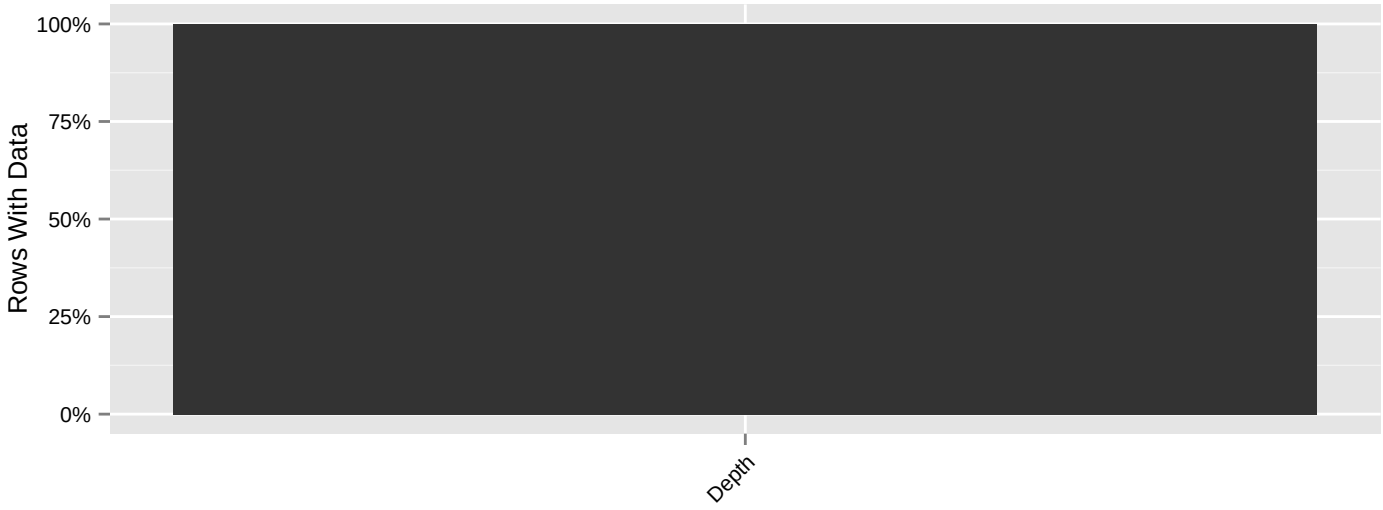

Figure 24: Segments with predictor values for the Bryde's whale Climatological model, Surveyed Area. This plot is used to assess how many segments would be lost by including a given predictor in a model.

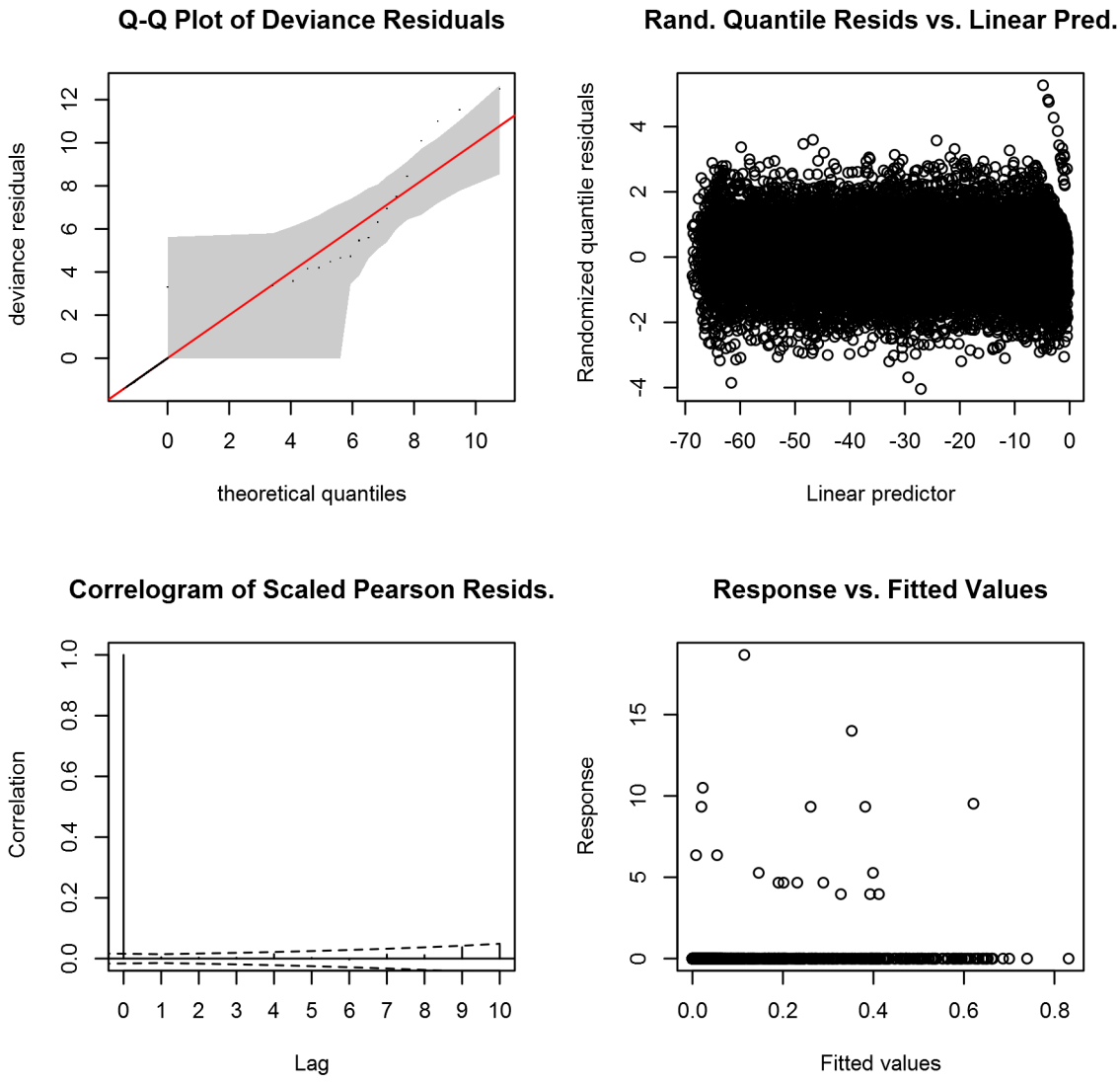

Figure 25: Statistical diagnostic plots for the Bryde's whale Climatological model, Surveyed Area.

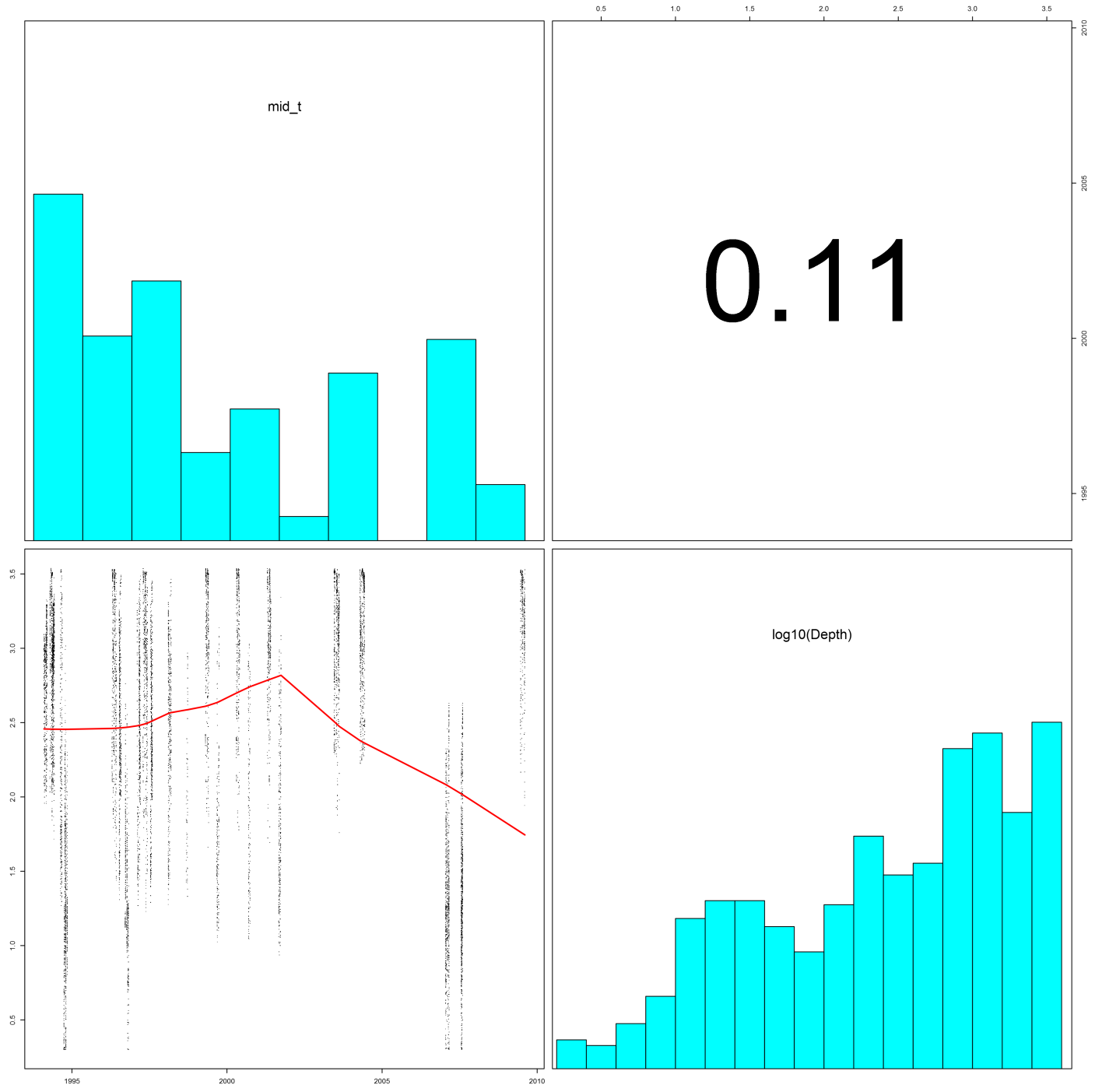

Figure 26: Scatterplot matrix for the Bryde's whale Climatological model, Surveyed Area. This plot is used to inspect the distribution of predictors (via histograms along the diagonal), simple correlation between predictors (via pairwise Pearson coefficients above the diagonal), and linearity of predictor correlations (via scatterplots below the diagonal). This plot is best viewed at high magnification.

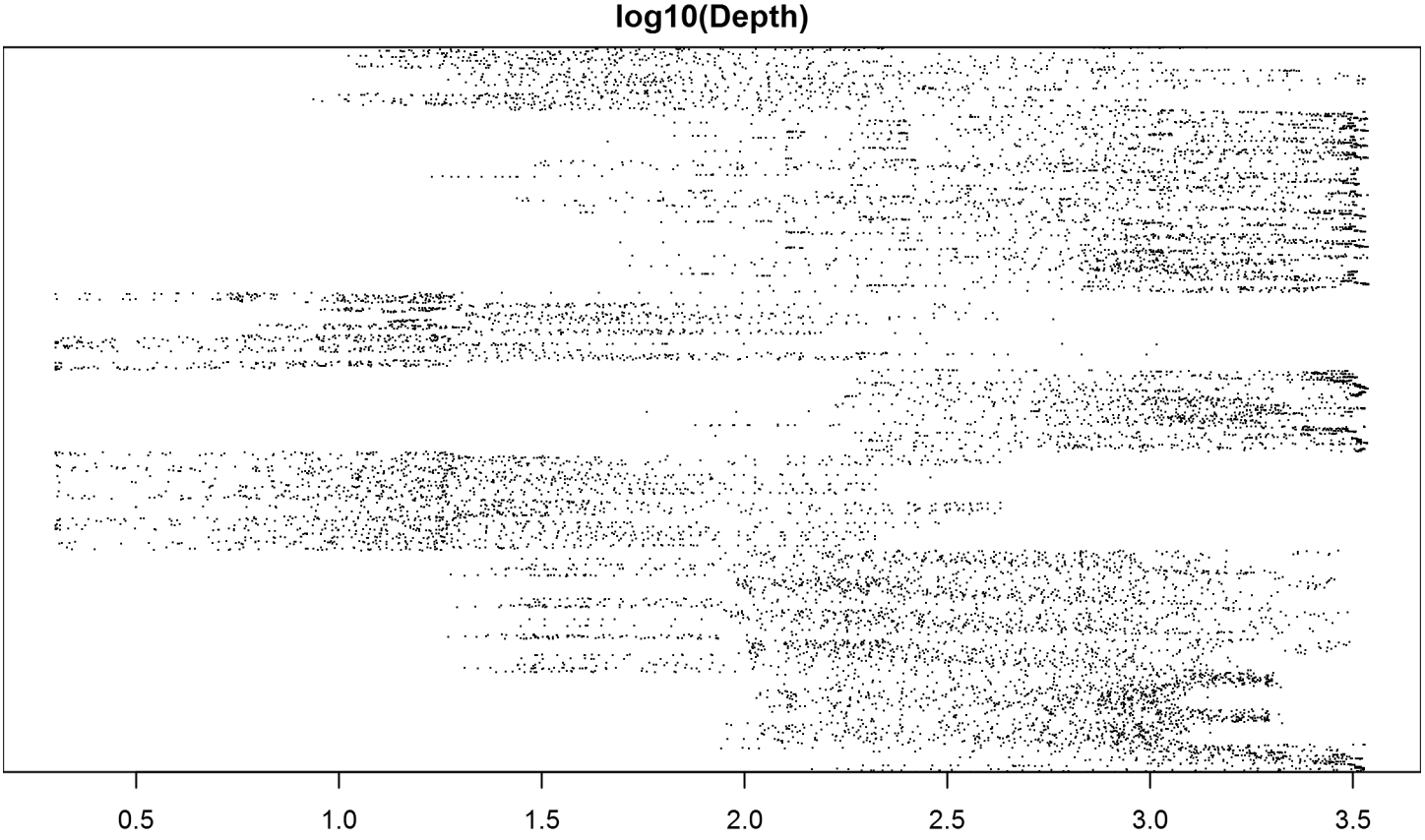

Figure 27: Dotplot for the Bryde's whale Climatological model, Surveyed Area. This plot is used to check for suspicious patterns and outliers in the data. Points are ordered vertically by transect ID, sequentially in time.

Model Comparison

Abundance Estimates

The table below shows the estimated mean abundance (number of animals) within the study area. The Assumed g(0)=1 column specifies whether the abundance estimate assumed that detection was certain along the survey trackline. Studies that assumed this did not correct for availability or perception bias, and therefore underestimated abundance. The In our models column specifies whether the survey data from the study was also used in our models. If not, the study provides a completely independent estimate of abundance.

Dates	Model or study	Estimated abundance	CV	Assumed g(0)=1	In our models
1994-2009	Climatological model	44	0.27	No	
2009	Oceanic waters, Jun-Aug (Waring et al. 2013)	33	1.07	Yes	Yes
2003-2004	Oceanic waters, Jun-Aug (Mullin 2007)	15	1.98	Yes	Yes
1996-2001	Oceanic waters, Apr-Jun (Mullin and Fulling 2004)	40	0.61	Yes	Yes
1991-1994	Oceanic waters, Apr-Jun (Hansen et al. 1995)	35	1.10	Yes	Yes

Table 16: Estimated mean abundance within the study area. For comparison, independent abundance estimates from NOAA technical reports and/or the scientific literature are shown. Please see the Discussion section below for our evaluation of our models compared to the other estimates. Note that our abundance estimates are averaged over the whole year, while the other studies may have estimated abundance for specific months or seasons. Our coefficients of variation (CVs) underestimate the true uncertainty in our estimates, as they only incorporated the uncertainty of the GAM stage of our models. Other sources of uncertainty include the detection functions and g(0) estimates. It was not possible to incorporate these into our CVs without undertaking a computationally-prohibitive bootstrap; we hope to attempt that in a future version of our models.

Density Map

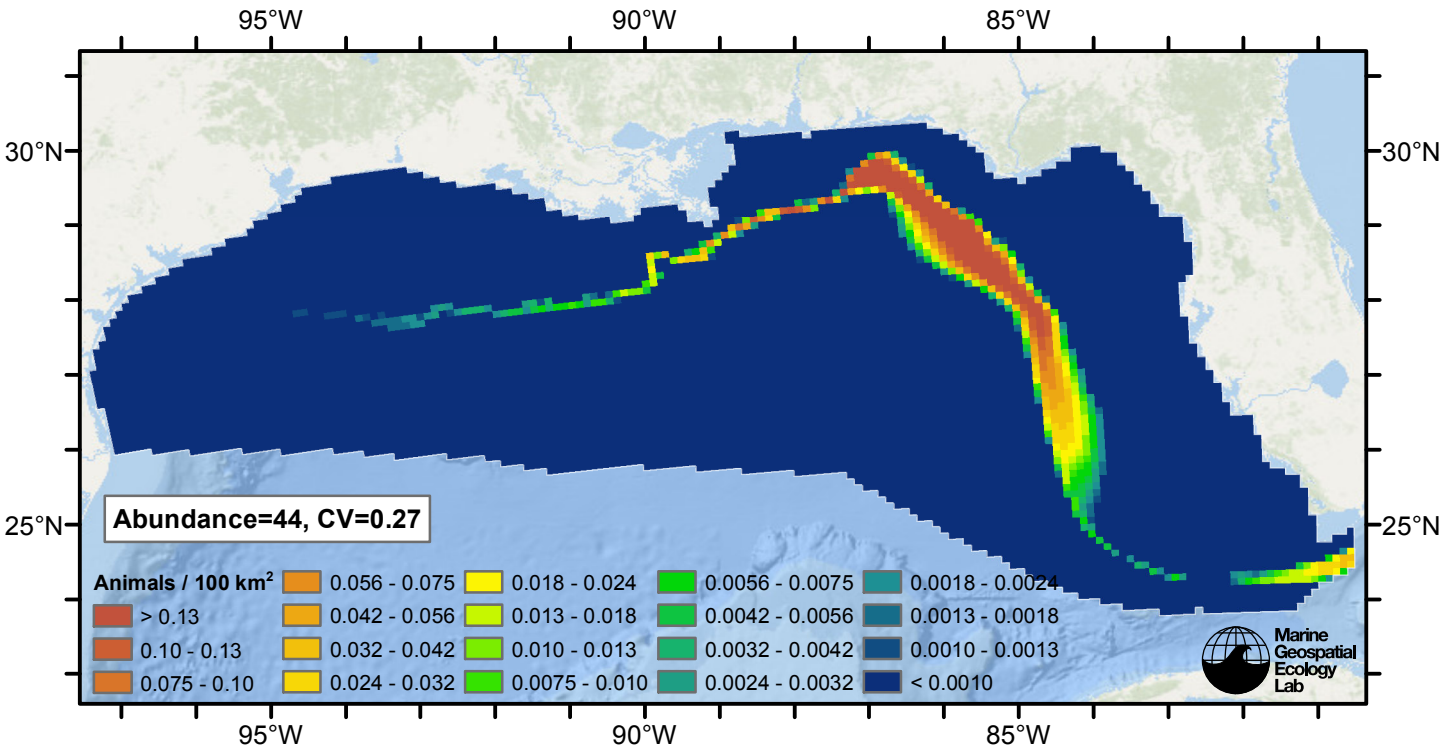

Figure 28: Bryde's whale density and abundance predicted by the climatological predictor model. Regions inside the study area (white line) where the background map is visible are areas we did not model (see text).

Discussion

Our two covariate model performed relatively well, explaining over 50% of the deviance in the data, owing to all of the sightings falling within a relatively narrow band of depths, as has been previously recognized (LaBrecque et al. 2015). Our total abundance estimate, 44, was higher than all of NOAA's estimates (see Abundance Estimates section above) but none of these estimates were statistically significantly different from each other, owing to the high uncertainty resulting from having so few sightings to work with.

We can offer several possible explanations for why our estimate was higher. First, as far as we know, NOAA did not include the ambiguous sightings in their model, while we did. By including these sightings, which were most likely Bryde's whales (Maze-Foley and Mullin 2006), and pooling the data over the entire study period (1994-2009), our result is more likely to reflect the true mean abundance of Bryde's whales over the entire study period, while NOAA's results are minimum abundance estimates for specific shorter periods.

Second, NOAA did not account for availability or perception bias, i.e. NOAA assumed that g(0)=1; we attempted to correct for these biases using available results from other regions (see g(0) Estimates section above), resulting in a higher estimate that would have occurred had we assumed that g(0)=1. As above, our approach results in an estimate that is more likely to reflect the true abundance of Bryde's whales, while NOAA's are minimum estimates.

Third, our detection functions showed a faster falloff in detectability with distance, compared to, for example, Mullin and Fulling (2004) and Mullin (2007). This resulted in a lower effective strip width in our study, which inflated the abundance value of each sighting relative to what resulted from NOAA's detection functions. We suspect the difference in detection functions may be traced to a difference in the proxy species added to Bryde's whales to obtain sufficient sightings to fit detection functions. NOAA restricted their detection functions to the data available from the particular surveys used to produce their estimates. In order to obtain sufficient sightings to fit a detection function, they included sperm whales with Bryde's whales. In contrast, we pooled many years of surveys together, and also drew on data available from surveys conducted on the U.S. east coast. Rather than including sperm whales, we included other species of baleen whales (see Detection Functions section above).

In our analyses of sperm whales and baleen whales, we found that sperm whales were significantly easier to detect. For example, our detection function for sperm whales sighted on the R/V Gordon Gunter surveys conducted in the Gulf of Mexico had an effective strip half width (ESHW) of 3806 m, while our detection function for baleen whales sighted by NOAA shipboard surveys conducted in the Gulf of Mexico or east coast (and applied in this Bryde's whale model) had an ESHW of only 1309 m. The much larger ESHW obtained for sperm whales reflects how much easier it is to detect them at a distance. In NOAA's analyses, Mullin and Fulling (2004) obtained an ESHW of 1913 m for sperm and Bryde's whales together, while Mullin (2007) obtained 3807 m. These ESHWs, larger than our baleen-whale-only estimate, caused NOAA to assume a larger area was effectively surveyed than we did, resulting in a lower abundance estimate for Bryde's whales.

A final possible reason that our abundance estimate exceeded NOAA's was that our prediction was based on a spatial model, while NOAA's were based on traditional line-transect estimates. The habitat predicted by our model might be too expansive–for example, Bryde's whales may not occur near the Florida Keys or west of the Mississippi River Delta, even though the model predicts them in these locations. We note that Bryde's whales may have historically occupied the northwestern Gulf (Reeves et al. 2011, Rosel and Wilcox 2014) and the the two sightings from 1992-1993 reported west of the Delta but not used in our model occurred within the narrow, westward-diminishing band of density predicted by our model. In any case, in the northwestern area where all of the sightings occurred in the 1994-2009 period, our model predicts density to be an order of magnitude or more higher than these more questionable areas. The maps presented in this report utilize an exponential scale that unintentionally obscures this difference.

In conclusion, we find our model to be a very credible density surface for the Gulf of Mexico Bryde's whale, given how little is known about this apparently-rare species, predicting highest density in the area they are believed to inhabit while remaining suitably parsimonious.

References

Barlow J (2006) Cetacean abundance in Hawaiian waters estimated from a summer/fall survey in 2002. Marine Mammal Science 22: 446-464.

Hansen LJ, Mullin KD, Roden CL (1995) Estimates of cetacean abundance in the northern Gulf of Mexico from vessel surveys. Southeast Fisheries Science Center, Miami Laboratory, Contribution No. MIA-94/95-25, 9 pp.

Hiby L (1999) The objective identification of duplicate sightings in aerial survey for porpoise. In: Marine Mammal Survey and Assessment Methods (Garner GW, Amstrup SC, Laake JL, Manly BFJ, McDonald LL, Robertson DG, eds.). Balkema, Rotterdam, pp. 179-189.

Jefferson TA, Schiro AJ (1997) Distribution of cetaceans in the offshore Gulf of Mexico. Mammal Rev. 27(1): 27-50.

Jefferson TA, Webber MA, Pitman RL (2008) Marine Mammals of the World: A Comprehensive Guide to Their Identification. Academic Press/Elsevier, 573 pp.

LaBrecque E, Curtice C, Harrison J, Van Parijs SM, Halpin PN (2015) Biologically Important Areas for Cetaceans Within U.S. Waters - Gulf of Mexico Region. Aquatic Mammals 41(1): 30-38.

Maze-Foley K, Mullin KD (2006) Cetaceans of the oceanic northern Gulf of Mexico: Distributions, group sizes and interspecific associations. J Cetacean Res Manage 8: 203-213.

Mullin KD (2007) Abundance of cetaceans in the oceanic Gulf of Mexico based on 2003-2004 ship surveys. 26 pp.

Mullin KD, Fulling GL (2004) Abundance of cetaceans in the oceanic northern Gulf of Mexico. Mar. Mamm. Sci. 20(4): 787-807.

Palka DL (2006) Summer Abundance Estimates of Cetaceans in US North Atlantic Navy Operating Areas. US Dept Commer, Northeast Fish Sci Cent Ref Doc. 06-03: 41 p.

Reeves RR, Lund JN, Smith TD, Josephson EA (2011) Insights from whaling logbooks on whales, dolphins, and whaling in the Gulf of Mexico. Gulf Mex Sci. 29: 41-67.

Rosel PE, Wilcox LA (2014) Genetic evidence reveals a unique lineage of Bryde's whales in the northern Gulf of Mexico. Endangered Species Research 25: 19-34.

Waring GT, Josephson E, Maze-Foley K, Rosel PE, eds. (2013) U.S. Atlantic and Gulf of Mexico Marine Mammal Stock Assessments – 2012. NOAA Tech Memo NMFS NE 223; 419 p.